Dual Caption Preference Optimization for Diffusion Models

Anonymous ACL submission

Abstract

Recent advancements in human preference optimization, originally developed for Large Language Models (LLMs), have shown significant potential in improving text-to-image diffusion models. These methods aim to learn the distribution of preferred samples while distinguishing them from less preferred ones. However, existing preference datasets often exhibit overlap between these distributions, leading to a *conflict distribution*. Additionally, we identified that input prompts contain irrelevant information for less preferred images, limiting the denoising network's ability to accurately predict noise in preference optimization methods, known as the *irrelevant prompt* issue. To address these challenges, we propose **Dual Caption Preference Optimization (DCPO)**, a novel approach that utilizes two distinct captions to mitigate irrelevant prompts. To tackle conflict distribution, we introduce the *Pick-Double Caption* dataset, a modified version of Pick-a-Pic v2 with separate captions for preferred and less preferred images. We further propose three different strategies for generating distinct captions: captioning, perturbation, and hybrid methods. Our experiments show that DCPO significantly improves image quality and relevance to prompts, outperforming other methods.

1 Introduction

Image synthesis models (Rombach et al., 2022; Esser et al., 2024) have achieved remarkable advancements in generating photo-realistic and high-quality images. Text-conditioned diffusion (Song et al., 2020a) models have led this progress due to their strong generalization abilities and proficiency in modeling high-dimensional data distributions. As a result, they have found wide range of applications in image editing (Brooks et al., 2023), video generation (Wu et al., 2023a) and robotics (Carvalho et al., 2023). Consequently, efforts have

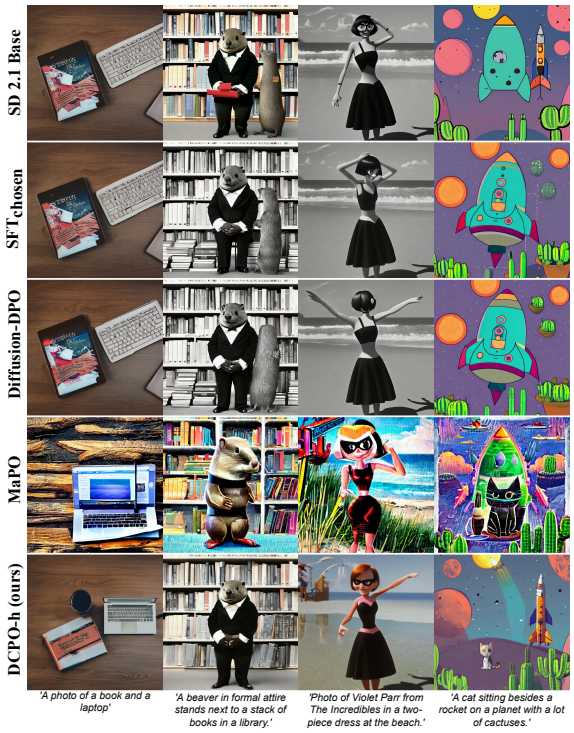

Figure 1: Sample image outputs generated by different methods from benchmarks of HPSv2, Geneval, and Pickscore. DCPO helps generate images that are notably better aligned with the prompts and also in higher visual appeal. See more examples in Appendix H.

focused on aligning them with human preferences, targeting specific attributes like safety (Liu et al., 2024b), style (Everaert et al., 2023), and personalization (Ruiz et al., 2023), thereby improving their usability and adaptability.

Similar to the alignment process of Large Language Models (LLMs), aligning diffusion models involves two main steps: **1.** Pre-training and **2.** Supervised Fine-Tuning (SFT). Recent fine-tuning based methods have been introduced to optimize diffusion models according to human preferences by leveraging Reinforcement Learning with Human Feedback (RLHF) (Ouyang et al., 2022), the aim of which is to maximize an explicit reward. However, challenges such as fine-tuning a separate

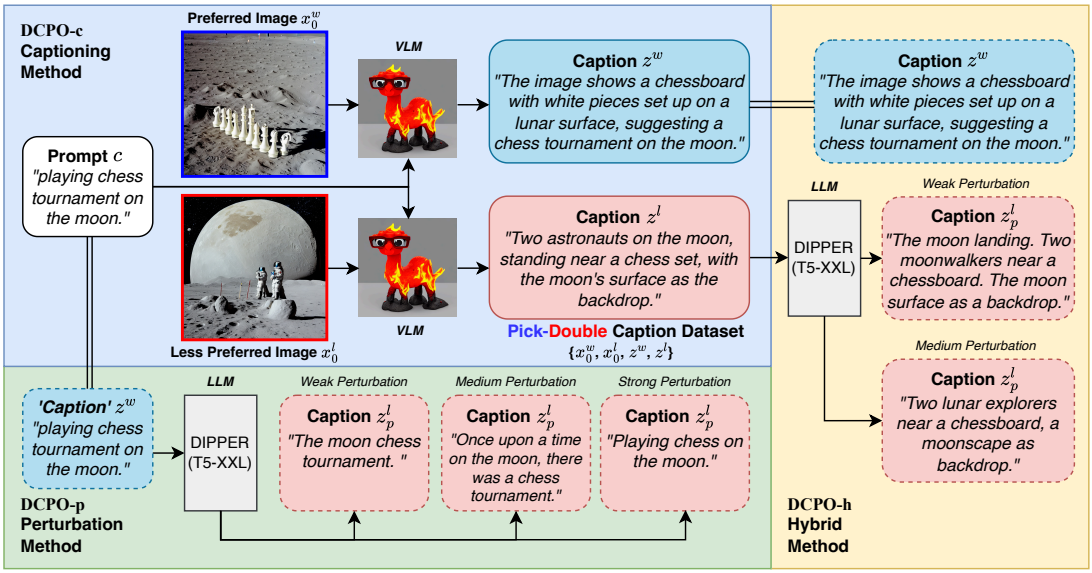

Figure 2: The DCPO pipeline in 3 variants: DCPO-c, DCPO-p, and DCPO-h, all of which require a duo of a captioned preferred image (x_0^w, z^w) and a captioned less-preferred image (x_0^l, z^l). **DCPO-c (Top Left):** We use a captioning model to generate distinctive captions respectively for images x_0^w and x_0^l given the shared prompt c. **DCPO-p (Bottom Left):** We take prompt c as the caption for image x_0^w, then we use a Large Language Model (LLM) to generate a semantically perturbed prompt z_p^l given prompt c as the caption for image x_0^l. **DCPO-h (Right):** A hybrid method where the generated caption z^l is now perturbed into z_p^l for image x_0^l. Our *Pick-Double Caption* Dataset discussed in Section 4.1 is constructed using DCPO-c.

reward model and reward hacking have led to the adoption of Direct Preference Optimization (DPO) (Rafailov et al., 2024) techniques like Diffusion-DPO (Wallace et al., 2024). Intuitively, Diffusion-DPO involves maximizing the difference between a preferred image and a less preferred image for a given prompt.

Although DPO-based methods are effective in comparison to SFT-based approaches, applying direct optimization in multi-modal settings presents certain challenges. Current preference optimization datasets consist of a preferred (x^w) and a less preferred (x^l) image for a given prompt (c). Ideally, x^w should show a higher correlation with c compared to x^l. However, we find that in current datasets, both the images share the same distribution for the given prompt c, which we refer to as *conflict distribution* in the data. Additionally, irrelative information in c restricts the U-Net's ability to predict noises from x^l in the diffusion reverse process, which we refer to as *irrelevant prompts*. This entails that there is a lack of sufficient distinguishing features between the two pairs (x^w, c), (x^l, c), thereby increasing the complexity of the optimization process.

To address the aforementioned bottleneck, we propose **DCPO: Dual Caption Preference Optimization**, a novel preference optimization technique designed to align diffusion models by utilizing two distinct captions corresponding to the preferred and less preferred image. DCPO broadly consists of two steps - a text generation framework that develops better aligned captions and a novel objective function that utilizes these captions as part of the training process.

The text generation framework seeks to alleviate the *conflict distribution* present in existing datasets. We hypothesize that c does not serve as the optimal signal for optimization because they do not convey the reasons why an image is preferred or dis-preferred; based on the above, we devise the following techniques to generate better aligned captions. The *first* method involves using a captioning model $Q_\phi(z^i|x^i, c)$; which generates a new prompt z^i based on an image x^i and the original prompt c, where $i \in (w, l)$. The *second* method introduces perturbation techniques f, such that $c = z^w, z^l = f(c)$; i.e. generating z^l, to represent the less preferred image, considering the original prompt c as the prompt aligned with the preferred image. We investigate multiple semantic variants of f, where each variant differs in the degree of perturbation applied to the original caption c. Finally, we also explore a hybrid com-

bination of the above methods, where we combine the strong prior of the captioning model and the efficient nature of the perturbation method. All the above methods are designed to generate captions that effectively discriminate between the preferred and less preferred images.

We introduce a novel objective function that allows DCPO to incorporate z^w and z^l into its optimization process. Specifically, during optimization, the policy model p_θ increases the likelihood of the preferred image x^w conditioned on the prompt z^w, while simultaneously decreasing the likelihood of the less preferred image x^l conditioned on the prompt z^l. The results in Tables 1 and 2 demonstrate that DCPO consistently outperforms other methods, with notable improvements of +0.21 in Pickscore, +0.45 in HPSv2.1, +1.8 in normalized ImageReward, +0.15 in CLIPscore, and +3% in GenEval. Additionally, DCPO achieved 58% in general preference and 66% in visual appeal compared to Diffusion-DPO on the PartiPrompts dataset, as evaluated by GPT-4o (see Figure 7).

In summary, our contributions are as follows :

Double Caption Generation. We introduce the Captioning and Perturbation methods to address the conflict distribution issue, as illustrated in Figure 3. In the Captioning method, we employ state-of-the-art models like LLaVA (Liu et al., 2024a) and Emu2 (Sun et al., 2024) to generate a caption z based on the image x and prompt c. Additionally, we use DIPPER (Krishna et al., 2024), a paraphrase generation model built by fine-tuning the T5-XXL model to create three levels of perturbation from the prompt c.

Dual Caption Preference Optimization (DCPO). We propose DCPO, a modified version of Diffusion-DPO, that leverages the U-Net encoder embedding space for preference optimization. This method enhances diffusion models by aligning them more closely with human preferences, using two distinct captions for the preferred and less preferred images during optimization.

Improved Model Performance. We demonstrate that our approach significantly outperforms SD 2.1, SFT, Diffusion-DPO, and MaPO across metrics such as Pickscore, HPSv2.1, GenEval, CLIPscore, normalized ImageReward, and GPT-4o (Achiam et al., 2023) evaluations.

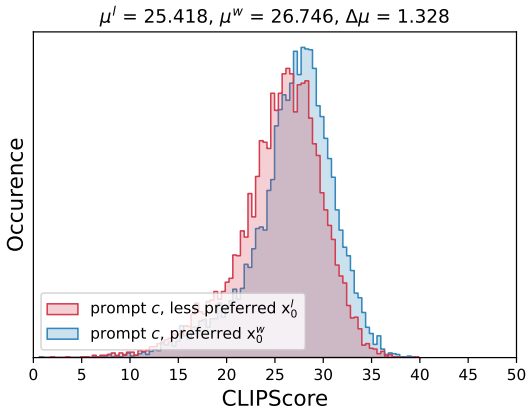

Figure 3: *Conflict distribution* in the Pick-a-Picv2 dataset. μ^l and μ^w are the average CLIPscores for preferred and less preferred images.

2 Related Works

Aligning Diffusion Models. Recent advances in preference alignment methods of text-to-image diffusion models have shown that reinforcement learning-free (RL-free) methods (Yang et al., 2024; Li et al., 2024; Yuan et al., 2024; Gambashidze et al., 2024; Park et al., 2024) outperform RL-based approaches (Fan and Lee, 2023; Fan et al., 2023; Hao et al., 2023; Lee et al., 2023; Prabhudesai et al., 2024; Black et al., 2024; Clark et al., 2024) mainly because they eliminate the need for an explicit reward model. Diffusion-DPO (Wallace et al., 2024) directly adopts the DPO method (Rafailov et al., 2024) into text-to-image diffusion models, using pairwise preference datasets as alignment guidance. Diffusion-KTO (Li et al., 2024) incorporates Kahneman & Tversky model of human utility to align these models, simplifying the process by using images with binary feedback signals in terms of likes or dislikes, instead of pairwise preference data. For better flexibility, Hong et al. (2024) introduce MaPO, an alignment technique independent of a reference model previously used by other methods, enabling greater control over stylistic adaptations. However, previous alignment methods optimize diffusion models based on a single prompt for a pair of images, which supports the *irrelevant prompts* issue explored in Section 3.1.

Text-to-image Preference Datasets. Text-to-image image preference datasets commonly involve the text prompt to generate the images, and two or more images are ranked according to human preference. HPS (Wu et al., 2023c) and HPSv2 (Wu et al., 2023b) create multiple im-

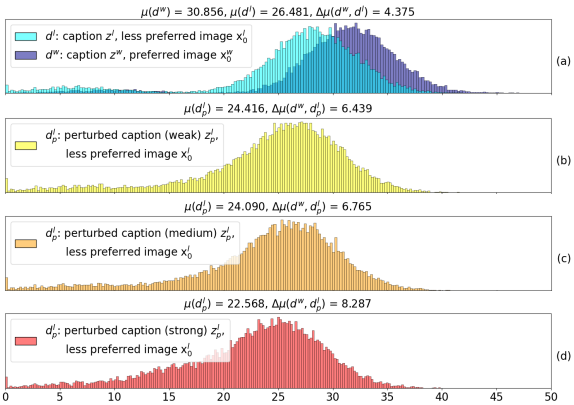

Figure 4: Effect of perturbation on semantic distributions (CLIPScore): **(a)** shows z^w and z^l distributions from LLaVA, while **(b-d)** depict increasing perturbation levels on z^l, amplifying the distribution gap. See Appendix E for details.

ages using a series of image generation models for a single prompt, and the images are ranked according to real-world human preferences. Moreover, a classifier is trained using the gathered preference dataset, which can be used as a metric for image-aligning tasks. Also, Pick-a-Pic v2 (Kirstain et al., 2023) follows a similar structure to create a pairwise preference dataset along with their CLIP (Radford et al., 2021) based scoring function, Pickscore. While these datasets are carefully created, having only one prompt for both or all the images introduces *conflict distribution*, which will be further discussed in Section 3.1. For this reason, we modified the Pick-a-Pic v2 dataset using recaptioning and perturbation methods to improve image alignment performance.

3 Method

In this section, we present the *conflict distribution* issue in preference datasets, where preferred and less-preferred images generated from the same prompt c exhibit significant overlap. We also explain the *irrelevant prompt* issue found in previous direct preference optimization methods. To address these challenges, we propose **Dual Caption Preference Optimization (DCPO)**, a method that uses distinct captions for preferred and less preferred images to improve diffusion model alignment.

3.1 The Challenges

Generally, to optimize a Large Language Model (LLM) using preference algorithms, we need a dataset $D = \{c, y^w, y^l\}$, where y^w and y^l represent the preferred and less preferred responses to a given prompt c. Ideally, the distributions of these responses should differ significantly. Similarly, in diffusion model alignment, the distributions of preferred and less preferred images should be distinct for the same prompt c. However, our analysis shows a substantial overlap between these distributions, which we call *conflict distribution*, as illustrated in Figure 3.

Another issue emerges when direct preference optimizes a diffusion model. In the reverse denoising process, the U-Net model predicts noise for both preferred and less preferred images using the same prompt c. As prompt c is more relevant to the preferred image, it becomes less effective for predicting the less preferred one, leading to reduced performance. We call this the *irrelevant prompts* problem.

3.2 DCPO: Dual Caption Preference Optimization

Motivated by the *conflict distribution* and *irrelevant prompts* issues, we propose DCPO, a new preference optimization method that optimizes diffusion models using two distinct captions. DCPO is a refined version of Diffusion-DPO designed to address these challenges. More details are in Appendix B. [1]

We start with a fixed dataset $D = \{c, x_0^w, x_0^l\}$, where each entry contains a prompt c and a pair of images generated by a reference model p_{ref}. The human labels indicate a preference, with x_0^w preferred over x_0^l. We assume the existence of a model $R_\phi(z|c, x)$, which generates a caption z given a prompt c and an image x. Using this model, we transform the dataset into $D' = \{z^w, z^l, x_0^w, x_0^l\}$, where z^w and z^l are captions for the preferred image x_0^w and the less-preferred image x_0^l, respectively. Our goal is to train a new model p_θ, aligned with human preferences, to generate outputs that are more desirable than those produced by the reference model.

The objective of RLHF is to maximize the reward $r(c, x_0)$ for the reverse process $p_\theta(x_{0:T}|z)$, while maintaining alignment with the original reference reverse process distribution. Building on prior work (Wallace et al., 2024), the DCPO objective is defined by direct optimization through the conditional distribution $p_\theta(x_{0:T}|z)$ as follows:

[1] For additional background about diffusion and preference optimization, refer to Appendix A.

$$\mathcal{L}_{\text{DCPO}}(\theta) = -\mathbb{E}_{(x_0^w, x_0^l)\sim\mathcal{D}'} \log\sigma\Big[\beta\mathbb{E}_{x_{1:T}^w\sim p_\theta(x_{1:T}^w|x_0^w,z^w), x_{1:T}^l\sim p_\theta(x_{1:T}^l|x_0^l,z^l)} \Big(\log\frac{p_\theta(x_{0:T}^w|z^w)}{p_{\text{ref}}(x_{0:T}^w|z^w)} - \log\frac{p_\theta(x_{0:T}^l|z^l)}{p_{\text{ref}}(x_{0:T}^l|z^l)}\Big)\Big] \quad (1)$$

where $\log[\cdot]$ is the sigmoid function.

However, as noted in Diffusion-DPO (Wallace et al., 2024), the sampling process $x_{1:T} \sim p(x_{1:T}|x_0)$ is inefficient and intractable. To overcome this, we follow a similar approach by applying Jensen's inequality and utilizing the convexity of the $-\log(\cdot)$ function to bring the expectation outside. By approximating the reverse process $p_\theta(x_{1:T}|x_0, z)$ with the forward process $q(x_{1:T}|x_0)$, and through algebraic manipulation and simplification, the DCPO loss can be expressed as:

$$\mathcal{L}_{\text{DCPO}}(\theta) = -\mathbb{E}_{(x_0^w,x_0^l)\sim\mathcal{D}', t\sim\mu(0,T), x_t^w\sim q(x_t^w|x_0^w), x_t^l\sim q(x_t^l|x_0^l)} \log\sigma\Big[-\beta T w(\lambda_t) \Big((||\epsilon^w - \epsilon_\theta(x_t^w, z^w, t)||_2^2 - ||\epsilon^w - \epsilon_{\text{ref}}(x_t^w, z^w, t)||_2^2) - (||\epsilon^l - \epsilon_\theta(x_t^l, z^l, t)||_2^2 - ||\epsilon^l - \epsilon_{\text{ref}}(x_t^l, z^l, t)||_2^2)\Big)\Big] \quad (2)$$

where $x_t^* = \alpha_t x_0^* + \sigma_t \epsilon^*$, and $\epsilon^* \sim \mathcal{N}(0, I)$ is a sample drawn from $q(x_t^*|x_0^*)$. $\lambda_t = \alpha_t^2/\sigma_t^2$ represents the signal-to-noise ratio, and $\omega(\lambda_t)$ is a weighting function.

To optimize a diffusion model using DCPO, a dataset $D = \{z^w, z^l, x_0^w, x_0^l\}$ is required, where captions are paired with the images. However, the current preference dataset only contains prompts c and image pairs without captions. To address this, we propose three methods for generating captions z and introduce a new high-quality dataset, *Pick-Double Caption*, which provides specific captions for each image, based on Pick-a-Pic v2 (Kirstain et al., 2023).

3.2.1 DCPO-c: Captioning Method

In this method, the captioning model $Q_\phi(z|c, x)$ generates the caption z based on the image x and the original prompt c. As a result, we obtain a preferred caption $z^w \sim Q_\phi(z^w|c, x^w)$ for the preferred image and a less preferred caption $z^l \sim Q_\phi(z^l|c, x^l)$ for the less preferred image, as illustrated in a sample in Figure 2. Thus, based on the generated captions z^w and z^l, we can optimize a diffusion model using the DCPO method.

In the experiment section, we evaluate the performance of DCPO-c and demonstrate that this method effectively mitigates the *conflict distribution* by creating two differentiable distributions. However, the question of how much divergence is needed between the two distributions remains. To investigate this, we propose Hypothesis 1.

Hyphothesis 1. *Let $d(z, x)$ represent the semantic distribution between a caption z and an image x, with μ being the mean of the distribution d, and $\Delta\mu = \mu(d(z_0^w, x_0^w)) - \mu(d(z_0^l, x_0^l))$ as the difference between the two distributions. Increasing $\Delta\mu$ between the preferred and less-preferred image distributions in a preference dataset beyond a threshold t (i.e., $\Delta\mu > t$), can improve the performance of the model p_θ.*

Our hypothesis suggests that increasing the distance between the two distributions up to a certain threshold t can improve alignment performance. To examine this, we propose the perturbation method to control the distance between the two distributions, represented by $\Delta\mu$.

3.2.2 DCPO-p: Perturbation Method

While using a captioning model is an effective way to address the *conflict distribution*, it risks deviating from the original distribution of prompt c, and the distributions of preferred and less preferred images may still remain close. To tackle these issues, we propose a perturbation method. In this approach, we assume that prompt c is highly relevant to the preferred image x_0^w and aim to generate a less relevant caption, denoted as c_p, based on prompt c. To achieve this, we use the model $W_\phi(c_p|c)$, which generates a perturbed version of prompt c, altering its semantic meaning. In this framework, prompt c corresponds to the preferred caption z^w ($c = z^w$), while the perturbed prompt c_p represents the less-preferred caption z^l ($c_p = z^l$). For the perturbation model W_ϕ, we utilized the DIPPER model (Krishna et al., 2024) built by fine-tuning the T5-XXL (Chung et al., 2022) to produce a degraded version of the prompt c.

We define three levels of perturbation: **1) Weak:** where prompt c_p has high semantic similarity to prompt c, with minimal differences. **2) Medium:** where the semantic difference between prompt c_p and c is more pronounced than in the weak level. **3) Strong:** where the majority of the semantics in prompt c_p differ significantly from prompt c. For further details on

the perturbation method, see Appendix E.

The main advantage of DCPO-p is to reduce the captioning process cost while staying closer to the original data distribution by using prompt c as the preferred caption. However, we observe that the quality of captions in DCPO-c outperforms that of the original prompt c, as shown in Table 8 in Appendix D. Based on this observation, we propose a hybrid method to improve the alignment performance by combining captioning and perturbation techniques.

3.2.3 DCPO-h: Hybrid Method

In this method, instead of perturbing the prompt c, we perturb the caption z generated by the model $Q_\phi(z|x, c)$ based on the image x and prompt c. As discussed in Section 3.2.1, the goal of the perturbation method is to increase the distance between the two distributions. However, the correlation between the image x_0 and prompt c significantly impacts alignment performance. Therefore, we propose Hypothesis 2.

Hypothesis 2. *Let $S(c, x)$ represent the correlation score between prompt c and image x, and $P(p_\theta(c_1, c_2))$ denote the performance of model p_θ optimized on captions c_1 and c_2 with DCPO, where W_ϕ is the perturbation model. If $S(z, x) > S(c, x)$, then $P(p_\theta(z^w, z_p^w \sim W_\phi(z_p^w|z^w))) > P(p_\theta(c, c_p \sim W_\phi(c_p|c)))$.*

In Section 4.3, we provide experimental evidence supporting Hypothesis 2 and investigate the potential of using $z_p^l \sim W_\phi(z_p^l|z^l)$ as the less-preferred caption z^l, instead of $z_p^w \sim W_\phi(z_p^w|z^w)$ as originally proposed in Hypothesis 2.

4 Experiments

We fine-tuned the U-Net model of Stable Diffusion (SD) 2.1 using DCPO on the *Pick-Double Caption* dataset and compared it with SD 2.1 models fine-tuned with $\text{SFT}_{\text{Chosen}}$, Diffusion-DPO, and MaPO on Pick-a-Picv2 in various metrics. We first describe the *Pick-Double Caption* dataset and compare it to Pick-a-Picv2. Subsequently, we provide an in-depth analysis of the results. Details on fine-tuning are in Appendix F, and further comparisons are in Appendix C.

4.1 Pick-Double Caption Dataset

Motivated by the *conflict distribution* observed in previous preference datasets, we applied the captioning method described in Section 3.2.1 to generate unique captions for each image in the Pick-a-Pic v2 dataset. For the *Pick-Double Caption* dataset, we sampled 20,000 instances from Pick-a-Pic v2 and cleaned the samples as detailed in Appendix D. We then employed two state-of-the-art captioning models, LLaVa-1.6-34B and Emu2-37B, to generate captions for both the preferred and less preferred images, as shown in Figure 2.

	Pick Score (↑)	HPSv2.1 (↑)	Image Reward (↑)	CLIP Score (↑)
Results from other methods				
SD 2.1	20.30	25.17	55.8	26.84
$\text{SFT}_{\text{Chosen}}$	20.35	25.09	56.4	26.98
Diffusion-DPO	20.36	25.10	56.4	26.98
MaPO	19.41	24.47	50.4	24.82
Results from our methods				
DCPO-c (LLaVA)	20.46	25.10	56.5	27.00
DCPO-c (Emu2)	20.46	25.06	56.6	26.97
DCPO-p	20.28	25.42	54.2	26.98
DCPO-h (LLaVA)	**20.57**	**25.62**	**58.2**	**27.13**

Table 1: Results on PickScore, HSPv2.1, ImageReward (normalized), and CLIPScore.

To generate the captions, we used two different prompting strategies: 1) **Conditional prompt:** where the model was explicitly instructed to generate a caption for image x based on the given prompt c, and 2) **Non-conditional prompt:** where the model provided a general description of the image in one sentence without referring to a specific prompt. More details are in Appendix D.

We evaluated the captions generated by LLaVA and Emu2 using CLIPscore, which revealed several key insights. LLaVA produced captions that have more correlation with the images for both preferred and less preferred samples compared to Emu2 and the original captions, although LLaVA's captions were significantly longer (see Table 8 in Appendix D). Models fine-tuned on captions from the conditional prompt strategy outperformed those using the non-conditional approach, though the conditional prompt captions were twice as long. Interestingly, despite Emu2 generating much shorter captions, the models fine-tuned on Emu2 were comparable to those fine-tuned on the original prompts from Pick-a-Pic v2.

A key challenge is generating captions for the less preferred images using the captioning method. We observed that in both prompting strategies, the captions for the preferred images are more aligned with the original prompt c distribution. However, the non-conditional prompt strategy of-

[2]Note that we rerun all the models on the same seeds to have a fair comparison.

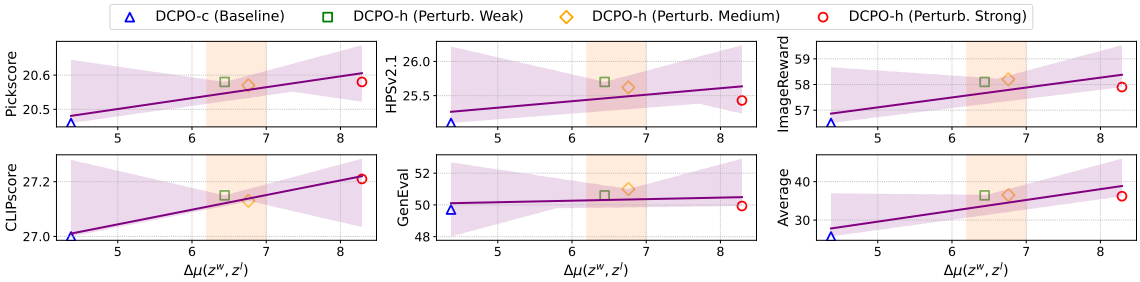

Figure 5: Performances in CLIPScore by four variants of DCPO-c and DCPO-h on different perturbation levels $\Delta\mu$. All the regression lines show that the performances peak when $\Delta\mu$ is around a threshold t (orange boundary).

ten produces captions for less preferred images that are out-of-distribution (OOD) from the original prompt c in most cases. We will explore this further in Section 4.3.

Finally, we observe that the key advantage of the *Pick-Double Caption* dataset is the greater difference in CLIPscore ($\Delta\mu$) between preferred and less preferred images compared to the original prompts. Specifically, while the original prompt has a $\Delta\mu$ of **1.3**, LLaVA shows a much larger difference at **4.3**, and Emu2 at **2.8**. This increased gap reflects improved alignment performance in models fine-tuned on this dataset, indicating that the captioning method mitigates the *conflict distribution*.

4.2 Performance Comparisons

We evaluated all methods on 2,500 unique prompts from the Pick-a-Picv2 (Kirstain et al., 2023) dataset, measuring performance using Pickscore (Kirstain et al., 2023), CLIPscore (Hessel et al., 2022), and Normalized ImageReward (Xu et al., 2023). Additionally, we generated images from 3,200 prompts in the HPSv2 (Wu et al., 2023b) benchmark and evaluated them using the HPSv2.1 model. To provide a comprehensive evaluation, we also compared the methods using GenEval (Ghosh et al., 2023), focusing on how well the fine-tuned models generated images with the correct number of objects, accurate colors, and proper object positioning.

We compared different versions of DCPO, including the captioning (DCPO-c), perturbation (DCPO-p), and hybrid (DCPO-h) methods, with other approaches, as outlined in Section 3.2. For more information on the fine-tuning process of the models, refer to Appendix F.

The results in Tables 1 and 2 show that DCPO-h significantly outperforms the best scores from other methods, with improvements of **+0.21** in Pickscore, **+0.45** in HPSv2.1, **+1.8** in ImageReward, **+0.15** in CLIPscore, and **+3%** in GenEval. Additionally, the results demonstrate that DCPO-c outperforms all other methods on GenEval, Pickscore, and CLIPscore. While DCPO-p performs slightly worse than DCPO-c, it still exceeds SD 2.1, SFT, Diffusion-DPO, and MaPO on GenEval. However, its scores on ImageReward and Pickscore suggest that it underperforms compared to the other approaches. Importantly, DCPO-p shows significant improvement over the other methods on HPSv2.1, highlighting the effectiveness of the perturbation method.

Method	Overall	Single object	Two objects	Counting	Colors	Position	Attribute binding
Results from other methods							
SD 2.1[2]	0.4775	0.96	**0.52**	0.35	0.80	**0.09**	0.15
$\text{SFT}_{\text{Chosen}}$	0.4797	**1.00**	0.42	0.42	0.81	0.07	0.14
Diffusion-DPO	0.4857	0.99	0.48	0.46	0.83	0.04	0.11
MaPO	0.4106	0.98	0.40	0.28	0.66	0.06	0.09
Results from our methods							
DCPO-c (LLaVA)	0.4971	**1.00**	0.43	0.53	**0.85**	0.02	0.14
DCPO-c (Emu2)	0.4925	**1.00**	0.41	0.50	**0.85**	0.04	0.15
DCPO-p	0.4906	**1.00**	0.41	0.50	0.83	0.03	**0.17**
DCPO-h (LLaVA)	**0.5100**	0.99	0.51	**0.54**	0.84	0.05	0.14

Table 2: Results on the GenEval Benchmark.

4.3 Ablation Studies and Analysis

Support of Hypothesis 1. As described in Section 3.2.2, we defined three levels of perturbation: weak, medium, and strong. In Hypothesis 1, we proposed that increasing the distance between the distributions of preferred and less preferred images $\Delta\mu$ improves model alignment performance. To explore this, we fine-tuned SD 2.1 using the DCPO-h method with three levels of perturbation applied to the less preferred captions z^l generated by LLaVA. The results in Figure 5 show that increasing the distance $\Delta\mu$ between the two distributions enhances performance. However, this distance must be controlled and kept below a threshold t, a hyperparameter that may vary depending on the task. These findings support our hypothesis.

Support of Hypothesis 2. To illustrate the impact of the correlation between the prompt c and

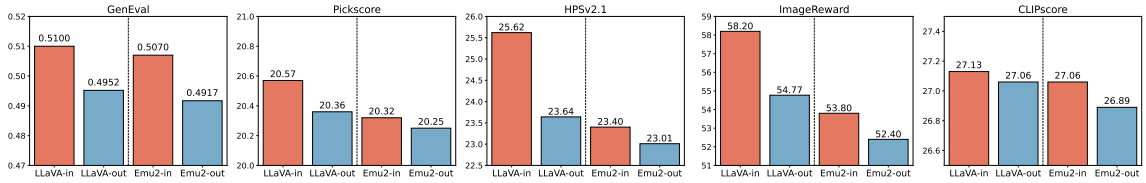

Figure 6: Comparisons of DCPO-h's performances over In-distribution vs. out-of-distribution data.

image x on the perturbation method, we perturbed both the original prompt c and the less preferred caption z^w, generated by the model Q_ϕ, where $z^w \sim W_\phi(z^w|Q_\phi(z^w|x^w, c))$. At the same time, we kept the caption generated by Q_ϕ for the preferred image as the preferred caption, $z^w \sim Q(z^w|x^w, c)$. In this case, we assume $Q_\phi =$ LLaVA and $W_\phi =$ DIPPER. The results in Table 8 in Appendix D show that the caption z generated by LLaVA is more correlated with the image x than the original prompt c, indicating that $S(z, x) > S(c, x)$. Based on the results in Table 3 in Appendix C, we conclude that perturbing more correlated captions leads to better performance.

In- vs. Out-of Distribution. We evaluated DCPO on in-distribution and out-of-distribution (OOD) data. As discussed in Section 4.1, the captioning model can generate OOD captions. To explore this, we fine-tuned SD 2.1 with DCPO-h using LLaVA and Emu2 captions at a medium perturbation level. Figure 6 Left shows that in-distribution data significantly improve alignment performance, while OOD results for LLaVA in GenEval, Pickscore, and CLIPscore are comparable to Diffusion-DPO. Similar behavior was observed for DCPO-c, as noted in Appendix F.

Effectiveness of the DCPO. Our analysis shows that LLaVA captions are twice the length of the original prompt c, raising the question of *whether DCPO's improvement is due to data quality or the optimization method*. To explore this, we fine-tuned SD 2.1 with Diffusion-DPO using LLaVA and Emu2 captions instead of the original prompt. The results in Table 4 in Appendix C show that models fine-tuned on LLaVA captions outperform Diffusion-DPO with the original prompt. However, DCPO-h still surpasses the new Diffusion-DPO models, demonstrating the effectiveness of the proposed optimization algorithm.

DCPO-h vs Diffusion-DPO on GPT-4o Judgment. We evaluated DCPO-h and Diffusion-DPO using GPT-4o on the PartiPrompts benchmark, consisting of 1,632 prompts. GPT-4o assessed images based on three criteria: **Q1)** General Preference (*Which image do you prefer given the prompt?*), **Q2)** Visual Appeal (*Which image is more visually appealing?*), and **Q3)** Prompt Alignment (*Which image better fits the text description?*). As shown in Figure 7, DCPO-h outperformed Diffusion-DPO in Q1 and Q2, with win rates of 58% and 66%. Refer to Appendix G for details on the prompt style and the analysis of position bias in GPT-4o judgments.

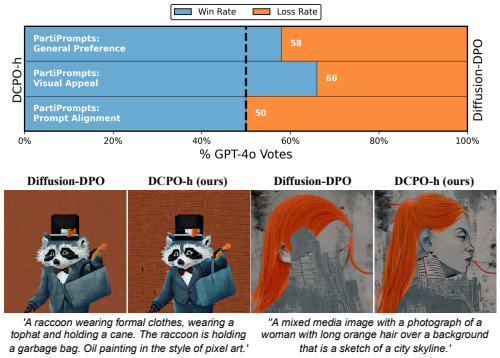

Figure 7: **(Top)** PartiPrompts benchmark results for three GPT-4o-voted questions. **(Bottom)** Qualitative comparison of DCPO-h and Diffusion-DPO.

5 Conclusion

In this paper, we present a novel preference optimization method for aligning text-to-image diffusion models called Dual Caption Preference Optimization (DCPO). We tackle two major challenges in previous preference datasets and optimization algorithms: the *conflict distribution* and *irrelevant prompt*. To overcome these issues, we introduce the *Pick-Double Caption* dataset, a modified version of the Pick-a-Pic v2 dataset. We also identify difficulties in generating captions, particularly the risk of out-of-distribution captions for images, and propose three approaches: 1) captioning (DCPO-c), 2) perturbation (DCPO-p), and 3) a hybrid method (DCPO-h). Our results show that DCPO-h significantly enhances alignment performance, outperforming methods like MaPO and Diffusion-DPO across multiple metrics.

Limitation

While DCPO achieves strong performance on various benchmarking metrics, its captioning and perturbation processes require considerable computational resources. We encourage future research to explore more efficient and cost-effective alternatives to further enhance its practicality. The preliminary results in Section C indicate that DCPO outperforms Diffusion-DPO across different backbones, such as Stable Diffusion XL (SDXL) (Podell et al., 2023). However, further investigation into its performance with emerging state-of-the-art models remains essential. Additionally, exploring DCPO's applications in safety-related tasks could be a valuable direction for future work. We believe our research will contribute significantly to the alignment community and inspire further advancements in this field.

Ethical Considerations

The authors state that this work is in accordance with the ACL Code of Ethics and does not raise ethical issues. AI assistants, specifically Grammarly and ChatGPT, were utilized to correct grammatical errors and restructure sentences.

References

Josh Achiam, Steven Adler, Sandhini Agarwal, Lama Ahmad, Ilge Akkaya, Florencia Leoni Aleman, Diogo Almeida, Janko Altenschmidt, Sam Altman, Shyamal Anadkat, et al. 2023. Gpt-4 technical report. *arXiv preprint arXiv:2303.08774*.

Hritik Bansal, Ashima Suvarna, Gantavya Bhatt, Nanyun Peng, Kai-Wei Chang, and Aditya Grover. 2024. Comparing bad apples to good oranges: Aligning large language models via joint preference optimization. *arXiv preprint arXiv:2404.00530*.

Kevin Black, Michael Janner, Yilun Du, Ilya Kostrikov, and Sergey Levine. 2024. Training diffusion models with reinforcement learning. In *The Twelfth International Conference on Learning Representations*.

Tim Brooks, Aleksander Holynski, and Alexei A Efros. 2023. Instructpix2pix: Learning to follow image editing instructions. In *Proceedings of the IEEE/CVF Conference on Computer Vision and Pattern Recognition*, pages 18392–18402.

Joao Carvalho, An T Le, Mark Baierl, Dorothea Koert, and Jan Peters. 2023. Motion planning diffusion: Learning and planning of robot motions with diffusion models. In *2023 IEEE/RSJ International Conference on Intelligent Robots and Systems (IROS)*, pages 1916–1923. IEEE.

Dimitrios Christodoulou and Mads Kuhlmann-Jørgensen. 2024. Finding the subjective truth: Collecting 2 million votes for comprehensive gen-ai model evaluation. *Preprint*, arXiv:2409.11904.

Hyung Won Chung, Le Hou, Shayne Longpre, Barret Zoph, Yi Tay, William Fedus, Eric Li, Xuezhi Wang, Mostafa Dehghani, Siddhartha Brahma, Albert Webson, Shixiang Shane Gu, Zhuyun Dai, Mirac Suzgun, Xinyun Chen, Aakanksha Chowdhery, Sharan Narang, Gaurav Mishra, Adams Yu, Vincent Zhao, Yanping Huang, Andrew Dai, Hongkun Yu, Slav Petrov, Ed H. Chi, Jeff Dean, Jacob Devlin, Adam Roberts, Denny Zhou, Quoc V. Le, and Jason Wei. 2022. Scaling instruction-finetuned language models. *arXiv preprint*.

Kevin Clark, Paul Vicol, Kevin Swersky, and David J. Fleet. 2024. Directly fine-tuning diffusion models on differentiable rewards. In *The Twelfth International Conference on Learning Representations*.

Patrick Esser, Sumith Kulal, Andreas Blattmann, Rahim Entezari, Jonas Müller, Harry Saini, Yam Levi, Dominik Lorenz, Axel Sauer, Frederic Boesel, et al. 2024. Scaling rectified flow transformers for high-resolution image synthesis. In *Forty-first International Conference on Machine Learning*.

Martin Nicolas Everaert, Marco Bocchio, Sami Arpa, Sabine Süsstrunk, and Radhakrishna Achanta. 2023. Diffusion in style. In *Proceedings of the IEEE/CVF International Conference on Computer Vision (ICCV)*, pages 2251–2261.

Ying Fan and Kangwook Lee. 2023. Optimizing DDPM sampling with shortcut fine-tuning. In *Proceedings of the 40th International Conference on Machine Learning*, volume 202 of *Proceedings of Machine Learning Research*, pages 9623–9639. PMLR.

Ying Fan, Olivia Watkins, Yuqing Du, Hao Liu, Moonkyung Ryu, Craig Boutilier, Pieter Abbeel, Mohammad Ghavamzadeh, Kangwook Lee, and Kimin Lee. 2023. DPOK: Reinforcement learning for fine-tuning text-to-image diffusion models. In *Advances in Neural Information Processing Systems*, volume 36, pages 79858–79885. Curran Associates, Inc.

Alexander Gambashidze, Anton Kulikov, Yuriy Sosnin, and Ilya Makarov. 2024. Aligning diffusion models with noise-conditioned perception. *Preprint*, arXiv:2406.17636.

Dhruba Ghosh, Hanna Hajishirzi, and Ludwig Schmidt. 2023. Geneval: An object-focused framework for evaluating text-to-image alignment. *Preprint*, arXiv:2310.11513.

Yaru Hao, Zewen Chi, Li Dong, and Furu Wei. 2023. Optimizing prompts for text-to-image generation. In *Thirty-seventh Conference on Neural Information Processing Systems*.

Jack Hessel, Ari Holtzman, Maxwell Forbes, Ronan Le Bras, and Yejin Choi. 2022. Clipscore: A reference-free evaluation metric for image captioning. *Preprint*, arXiv:2104.08718.

Jiwoo Hong, Sayak Paul, Noah Lee, Kashif Rasul, James Thorne, and Jongheon Jeong. 2024. Margin-aware preference optimization for aligning diffusion models without reference. *Preprint*, arXiv:2406.06424.

Diederik Kingma, Tim Salimans, Ben Poole, and Jonathan Ho. 2021. Variational diffusion models. *Advances in neural information processing systems*, 34:21696–21707.

Yuval Kirstain, Adam Polyak, Uriel Singer, Shahbuland Matiana, Joe Penna, and Omer Levy. 2023. Pick-a-pic: An open dataset of user preferences for text-to-image generation. In *Thirty-seventh Conference on Neural Information Processing Systems*.

Kalpesh Krishna, Yixiao Song, Marzena Karpinska, John Wieting, and Mohit Iyyer. 2024. Paraphrasing evades detectors of ai-generated text, but retrieval is an effective defense. *Advances in Neural Information Processing Systems*, 36.

Kimin Lee, Hao Liu, Moonkyung Ryu, Olivia Watkins, Yuqing Du, Craig Boutilier, Pieter Abbeel, Mohammad Ghavamzadeh, and Shixiang Shane Gu. 2023. Aligning text-to-image models using human feedback. *Preprint*, arXiv:2302.12192.

Shufan Li, Konstantinos Kallidromitis, Akash Gokul, Yusuke Kato, and Kazuki Kozuka. 2024. Aligning diffusion models by optimizing human utility. *Preprint*, arXiv:2404.04465.

Haotian Liu, Chunyuan Li, Qingyang Wu, and Yong Jae Lee. 2024a. Visual instruction tuning. *Advances in neural information processing systems*, 36.

Runtao Liu, Ashkan Khakzar, Jindong Gu, Qifeng Chen, Philip Torr, and Fabio Pizzati. 2024b. Latent guard: a safety framework for text-to-image generation. *arXiv preprint arXiv:2404.08031*.

Long Ouyang, Jeffrey Wu, Xu Jiang, Diogo Almeida, Carroll Wainwright, Pamela Mishkin, Chong Zhang, Sandhini Agarwal, Katarina Slama, Alex Ray, et al. 2022. Training language models to follow instructions with human feedback. *Advances in neural information processing systems*, 35:27730–27744.

Yong-Hyun Park, Sangdoo Yun, Jin-Hwa Kim, Junho Kim, Geonhui Jang, Yonghyun Jeong, Junghyo Jo, and Gayoung Lee. 2024. Direct unlearning optimization for robust and safe text-to-image models. *Preprint*, arXiv:2407.21035.

Dustin Podell, Zion English, Kyle Lacey, Andreas Blattmann, Tim Dockhorn, Jonas Müller, Joe Penna, and Robin Rombach. 2023. Sdxl: Improving latent diffusion models for high-resolution image synthesis. *Preprint*, arXiv:2307.01952.

Mihir Prabhudesai, Anirudh Goyal, Deepak Pathak, and Katerina Fragkiadaki. 2024. Aligning text-to-image diffusion models with reward backpropagation.

Alec Radford, Jong Wook Kim, Chris Hallacy, Aditya Ramesh, Gabriel Goh, Sandhini Agarwal, Girish Sastry, Amanda Askell, Pamela Mishkin, Jack Clark, Gretchen Krueger, and Ilya Sutskever. 2021. Learning transferable visual models from natural language supervision. *Preprint*, arXiv:2103.00020.

Rafael Rafailov, Archit Sharma, Eric Mitchell, Christopher D Manning, Stefano Ermon, and Chelsea Finn. 2024. Direct preference optimization: Your language model is secretly a reward model. *Advances in Neural Information Processing Systems*, 36.

Robin Rombach, Andreas Blattmann, Dominik Lorenz, Patrick Esser, and Björn Ommer. 2022. High-resolution image synthesis with latent diffusion models. In *Proceedings of the IEEE/CVF conference on computer vision and pattern recognition*, pages 10684–10695.

Sheldon M Ross. 2014. *Introduction to probability models*. Academic press.

Nataniel Ruiz, Yuanzhen Li, Varun Jampani, Yael Pritch, Michael Rubinstein, and Kfir Aberman. 2023. Dreambooth: Fine tuning text-to-image diffusion models for subject-driven generation. In *Proceedings of the IEEE/CVF conference on computer vision and pattern recognition*, pages 22500–22510.

John Schulman, Filip Wolski, Prafulla Dhariwal, Alec Radford, and Oleg Klimov. 2017. Proximal policy optimization algorithms. *arXiv preprint arXiv:1707.06347*.

Jiaming Song, Chenlin Meng, and Stefano Ermon. 2020a. Denoising diffusion implicit models. *arXiv:2010.02502*.

Yang Song, Conor Durkan, Iain Murray, and Stefano Ermon. 2021. Maximum likelihood training of score-based diffusion models. *Advances in neural information processing systems*, 34:1415–1428.

Yang Song and Stefano Ermon. 2019. Generative modeling by estimating gradients of the data distribution. *Advances in neural information processing systems*, 32.

Yang Song, Jascha Sohl-Dickstein, Diederik P Kingma, Abhishek Kumar, Stefano Ermon, and Ben Poole. 2020b. Score-based generative modeling through stochastic differential equations. *arXiv preprint arXiv:2011.13456*.

Quan Sun, Yufeng Cui, Xiaosong Zhang, Fan Zhang, Qiying Yu, Yueze Wang, Yongming Rao, Jingjing Liu, Tiejun Huang, and Xinlong Wang. 2024. Generative multimodal models are in-context learners. In *Proceedings of the IEEE/CVF Conference on Computer Vision and Pattern Recognition*, pages 14398–14409.

Bram Wallace, Meihua Dang, Rafael Rafailov, Linqi Zhou, Aaron Lou, Senthil Purushwalkam, Stefano Ermon, Caiming Xiong, Shafiq Joty, and Nikhil Naik. 2024. Diffusion model alignment using direct preference optimization. In *Proceedings of the IEEE/CVF Conference on Computer Vision and Pattern Recognition*, pages 8228–8238.

Jay Zhangjie Wu, Yixiao Ge, Xintao Wang, Stan Weixian Lei, Yuchao Gu, Yufei Shi, Wynne Hsu, Ying Shan, Xiaohu Qie, and Mike Zheng Shou. 2023a. Tune-a-video: One-shot tuning of image diffusion models for text-to-video generation. In *Proceedings of the IEEE/CVF International Conference on Computer Vision*, pages 7623–7633.

Xiaoshi Wu, Yiming Hao, Keqiang Sun, Yixiong Chen, Feng Zhu, Rui Zhao, and Hongsheng Li. 2023b. Human preference score v2: A solid benchmark for evaluating human preferences of text-to-image synthesis. *Preprint*, arXiv:2306.09341.

Xiaoshi Wu, Keqiang Sun, Feng Zhu, Rui Zhao, and Hongsheng Li. 2023c. Human preference score: Better aligning text-to-image models with human preference. In *Proceedings of the IEEE/CVF International Conference on Computer Vision*, pages 2096–2105.

Jiazheng Xu, Xiao Liu, Yuchen Wu, Yuxuan Tong, Qinkai Li, Ming Ding, Jie Tang, and Yuxiao Dong. 2023. Imagereward: Learning and evaluating human preferences for text-to-image generation. *Preprint*, arXiv:2304.05977.

Kai Yang, Jian Tao, Jiafei Lyu, Chunjiang Ge, Jiaxin Chen, Qimai Li, Weihan Shen, Xiaolong Zhu, and Xiu Li. 2024. Using human feedback to fine-tune diffusion models without any reward model. *Preprint*, arXiv:2311.13231.

Huizhuo Yuan, Zixiang Chen, Kaixuan Ji, and Quanquan Gu. 2024. Self-play fine-tuning of diffusion models for text-to-image generation. *Preprint*, arXiv:2402.10210.

A Preliminary

A.1 Diffusion Models

Based on samples from a data distribution $q(x_0)$, a noise scheduling function α_t and σ_t (Rombach et al., 2022) denoising diffusion models (Song et al., 2020b) are generative models $p_\theta(x_0)$ that operate through a discrete-time reverse process structured as a Markov Decision Proces where

$$p_\theta(x_{t-1}|x_t) = \mathcal{N}(x_{t-1}; \mu_\theta(x_t), \sigma^2_{t|t-1}\frac{\sigma^2_{t-1}}{\sigma^2_t}I). \tag{3}$$

The training process involves minimizing the evidence lower bound (ELBO) associated with this model (Song et al., 2021):

$$L_{DM} = \mathbb{E}_{x_0,\epsilon,t,x_t}[\omega(\lambda_t)||\epsilon - \epsilon_\theta(x_t, t)||^2_2] \tag{4}$$

where $\epsilon \sim \mathcal{N}(0, I)$, $t \sim \mathcal{U}(o, T)$, x_t $q(x_t|x_0) = \mathcal{N}(x_t; \alpha_t x_0, \sigma^2_t I).\lambda_t = \alpha^2_t/\sigma^2_t$ is a signal-to-noise ratio (Kingma et al., 2021), $\omega(\lambda_t)$ is a predefined weighting function (Song and Ermon, 2019).

A.2 Preference Optimization

Aligning a generative model typically involves fine-tuning it to produce outputs that are more aligned with human preferences. Estimating the reward model r based on human preference is generally challenging, as we do not have direct access to the reward model. However, if we assume the availability of ranked data generated under a given condition c, where $x^w_0 \succ x^l_0|c$ (with x^w_0 representing the preferred sample and x^l_0 the less-preferred sample), we can apply the Bradley-Terry theory to model these preferences. The Bradley-Terry (BT) model expresses human preferences as follows:

$$p_{BT}(x^w_0 \succ x^l_0|c) = \sigma(r(c, x^w_0) - r(c, x^l_0)) \tag{5}$$

where $\sigma(\cdot)$ is the sigmoid function, and $r(x_0, c)$ is derived from a neural network parameterized by ϕ.

Subsequently, ϕ is estimated by maximum likelihood training for binary classification as follows:

$$L_{BT}(\phi) = -\mathbb{E}_{c,x^w_0,x^l_0[\log\sigma(r_\phi(c,x^w_0)-r_\phi(c,x^l_0))]} \tag{6}$$

where prompt c and data pair (x^w_0, x^l_0) are sourced from a human-annotated dataset.

This approach to reward modeling has gained popularity in aligning large language models, particularly when combined with reinforcement learning (RL) techniques like proximal policy optimization (PPO) (Schulman et al., 2017) to fine-tune the model based on rewards learned from human preferences, known as Reinforcement Learning from Human Feedback (RLHF) (Ouyang et al., 2022). The goal of RLHF is to optimize the conditional distribution $p(x_0|c)$ (where $c \sim D_c$) such that the reward model $r(c, x_0)$ is maximized, while keeping the policy model within the desired distribution using a KL-divergence term to ensure it remains reachable under the following objective:

$$\max_{p_\theta} \mathbb{E}_{c\sim\mathcal{D}_c, x_0\sim p_\theta(x_0|c)}[r(c, x_0)] - \beta\mathbb{D}_{KL}[p_\theta(x_0|c)||p_{\text{ref}}(x_0|c)] \tag{7}$$

where β controls how far the policy model p_θ can deviate from the reference model p_{ref}.

It can be demonstrated that the objective in Equation 7 converges to the following policy model:

$$p^*_\theta(x_0|c) = p_{\text{ref}}(x_0|c)\exp(r(c, x_0)/\beta)/Z(c) \tag{8}$$

where Z is the partition function.

The training objective for p_θ, inspired by DPO, has been derived to be equivalent to Equation 8 without the need for an explicit reward model $r(x, c)$. Instead, RLHF learns directly from the preference data $(c, x^w_0, x^l_0) \sim D$:

$$L_{\text{DPO}}(\theta) = -\mathbb{E}_{c,x^w_0,x^l_0}\Big[\log\sigma\Big(\beta\log\frac{p_\theta(x^w_0|c)}{p_{\text{ref}}(x^w_0|c)} - \beta\log\frac{p_\theta(x^l_0|c)}{p_{\text{ref}}(x^l_0|c)}\Big)\Big] \tag{9}$$

where $\sigma(\cdot)$ is the sigmoid function.

Through this re-parameterization, instead of optimizing the reward function r before applying reinforcement learning, the RLHF method directly optimizes the conditional distribution $p_\theta(x_0|c)$.

B Formal Proofs Regarding DCPO

B.1 Optimizing the DCPO Loss is Optimizing the DPO Loss

Inspired by Bansal et al. (2024), we can intuitively assume that the DCPO objective is to learn an aligned model p_θ by weighting the joint probability of preferred images $p_\theta(x_0^w, z^w)$ over less preferred images $p_\theta(x_0^l, z^l)$. We set the optimization objective of DCPO is to minimize the following:

$$\begin{aligned}\mathcal{L}_{\text{DCPO}}(\theta) = -\mathbb{E}_{(x_0^w, x_0^l, z^l, z^w)\sim\mathcal{D}'} \log \sigma(\beta \mathbb{E}_{x_{1:T}^w \sim p_\theta(x_{1:T}^w|x_0^w, z^w), x_{1:T}^l \sim p_\theta(x_{1:T}^l, x_0^l, z^l)} \\ [\log \frac{p_\theta(x_{0:T}^w, z^w)}{p_{\text{ref}}(x_{0:T}^w, z^w)} - \log \frac{p_\theta(x_{0:T}^l, z^l)}{p_{\text{ref}}(x_{0:T}^l|z^l)}])\end{aligned} \tag{10}$$

Here, we highlight that reducing $\mathcal{L}_{\text{DCPO}}(\theta)$ is equivalently reducing $\mathcal{L}_{\text{DPO}}(\theta)$ when the captions are the same for the preferred and less preferred images.

Lemma 1. *Under the case where $\mathcal{D}_{define} = \{x_0^w, c, x_0^l, c\}$, that is, the image captions are identical for the given pair of preferred and less preferred images (x_0^w, x_0^l), we have $L_{DPO}(\theta; \mathcal{D}_{DPO}; \beta; p_{ref}) = L_{DCPO}(\theta; \mathcal{D}_{define}; \beta; p_{ref})$, in which $\mathcal{D}_{DPO} = \{c, x_0^w, x_0^l\}$.*

Proof of Lemma 1.

$$\begin{aligned}\mathcal{L}_{\text{DCPO}}(\theta; \mathcal{D}', \beta, p_{\text{ref}}) &= \mathbb{E}_{(x_0^w, x_0^l, z^w, z^l)\sim\mathcal{D}'} \\ &\left[\log\left(\sigma\left(\beta \log \frac{p_\theta(x_0^w, z^w)}{p_{\text{ref}}(x_0^w, z^w)} - \beta \log \frac{p_\theta(x_0^l, z^l)}{p_{\text{ref}}(x_0^l, z^l)}\right)\right)\right] \\ &= \mathbb{E}_{(x_0^w, x_0^l, z^w, z^l)\sim\mathcal{D}'} \\ &\left[\log\left(\sigma\left(\beta \log \frac{p_\theta(x_0^w|z^w)p_\theta(z^w)}{p_{\text{ref}}(x_0^w|z^w)p_{\text{ref}}(z^w)} \quad -\beta \log \frac{p_\theta(x_0^l|z^l)p_\theta(z^l)}{p_{\text{ref}}(x_0^l|z^l)p_{\text{ref}}(z^l)}\right)\right)\right]\end{aligned} \tag{11}$$

$$\begin{aligned}\mathcal{L}_{\text{DCPO}}(\theta; \mathcal{D}_{\text{define}}, \beta, p_{\text{ref}}) &\overset{z^w=z^l=c}{=} \mathbb{E}_{(x_0^w, c, x_0^l, c)\sim\mathcal{D}_{\text{define}}} \\ &\left[\log\left(\sigma\left(\frac{p_\theta(c)}{p_{\text{ref}}(c)}\left(\beta \log \frac{p_\theta(x_0^w|c)}{p_{\text{ref}}(x_0^w|c)} - \beta \log \frac{p_\theta(x_0^l|c)}{p_{\text{ref}}(x_0^l|c)}\right)\right)\right)\right] \\ &\overset{\frac{p_\theta(c)}{p_{\text{ref}}(c)}=C}{=} \mathbb{E}_{(x_0^w, x_0^l, c)\sim\mathcal{D}_{\text{DPO}}} \\ &\left[\log\left(\sigma\left(C \cdot \beta \log \frac{p_\theta(x_0^w|c)}{p_{\text{ref}}(x_0^w|c)} - C \cdot \beta \log \frac{p_\theta(x_0^l|c)}{p_{\text{ref}}(x_0^l|c)}\right)\right)\right] \\ &= \mathcal{L}_{\text{DPO}}(\theta; \mathcal{D}_{\text{DPO}}, \beta, p_{\text{ref}})\end{aligned} \tag{12}$$

In Equation 12, C is a constant value that equates to $\frac{p_\theta(c)}{p_{\text{ref}}(c)}$. The proof above follows the Bayes rule by substituting c according to $z^w = z^l = c$.

B.2 Analyses of DCPO's Effectiveness

In this section, we present the formal proofs of why our DCPO leads to a more optimized $L(\theta)$ of a Diffusion-based model and, consequently, better performance in preference alignment tasks.

Proof 1. *Increasing the difference between $\Delta_{preferred}$ and $\Delta_{less\text{-}preferred}$ improves the optimization of $L(\theta)$.*
For better clarity, the loss function $L(\theta)$ can be written as:

$$L(\theta) = -\mathbb{E}\left[\log \sigma\big(-\beta T \omega(\lambda_t) \cdot M\big)\right]$$

where $\sigma(x)$ is the sigmoid function that squashes its input x into the output range $(0, 1)$, and $M = \Delta_{\text{preferred}} - \Delta_{\text{less-preferred}}$, i.e., the margin between the respective importance of the preferred and less preferred predictions.

Characteristically, the gradient of $\sigma(x)$ is at its maximum near $x = 0$ and decreases as $|x|$ increases. A larger margin in terms of M makes it easier for the optimization to drive the sigmoid function towards its asymptotes, reducing loss.

- When M is small ($|M| \approx 0$): The sigmoid $\sigma(-\beta T \omega(\lambda_t) \cdot M)$ is near 0.5 (its midpoint). Also, the gradient of $\log \sigma(x)$ is the largest near this point, meaning the model struggles to differentiate between preferred and less preferred predictions effectively.

- When M is large ($|M| \gg 0$): The sigmoid $\sigma(-\beta T \omega(\lambda_t) \cdot M)$ moves closer to 0 or 1, depending on the sign of M. For a well-aligned model, if the preferred predictions are correct, $M > 0$ and $\sigma(-\beta T \omega(\lambda_t) \cdot M)$ approach 1, thus minimizing the loss.

Intuitively, an ideally large M represents a clear distinction between the preferred image-caption versus the less preferred image-caption. Thus, by maximizing M, we may push the loss $L(\theta)$ towards its minimum, leading to better soft-margin optimization.

Proof 2. *Replacing caption c with the specifically generated caption z^l for the less-preferred image $\mathbf{x}_0^l$ decreases $\Delta_{less\text{-}preferred}$.*

To analyze how replacing $\mathbf{c}$ with $\mathbf{z}^l$, where $\mathbf{c} \subset \mathbf{z}^l$ and $\mathbf{z}^l \sim Q(\mathbf{z}^l | x^l, c)$, for the less-preferred image $\mathbf{x}_0^l$ improves the optimization, we delve into how the loss function is affected by this substitution. The term relevant to the less-preferred image $\mathbf{x}_t^l$ in the loss is:

$$\Delta_{\text{less-preferred}} = \|\boldsymbol{\epsilon}^l - \boldsymbol{\epsilon}_\theta(\mathbf{x}_t^l, t, \mathbf{c})\|_2^2 - \|\boldsymbol{\epsilon}^l - \boldsymbol{\epsilon}_{\text{ref}}(\mathbf{x}_t^l, t, \mathbf{c})\|_2^2.$$

Replacing $\mathbf{c}$ with $\mathbf{z}^l$ modifies the predicted noise term $\boldsymbol{\epsilon}_\theta(\mathbf{x}_t^l, t, \mathbf{c})$ to $\boldsymbol{\epsilon}_\theta(\mathbf{x}_t^l, t, \mathbf{z}^l)$. Since $\mathbf{z}^l$ better represents $\mathbf{x}_t^l$, we have:

$$\|\boldsymbol{\epsilon}^l - \boldsymbol{\epsilon}_\theta(\mathbf{x}_t^l, t, \mathbf{z}^l)\|_2^2 < \|\boldsymbol{\epsilon}^l - \boldsymbol{\epsilon}_\theta(\mathbf{x}_t^l, t, \mathbf{c})\|_2^2 \tag{13}$$

When $\|\boldsymbol{\epsilon}^l - \boldsymbol{\epsilon}_\theta(\mathbf{x}_t^l, t, \mathbf{z}^l)\|_2^2$ becomes smaller, the term $\Delta_{\text{less-preferred}}$ decreases. This leads to $\Delta_{\text{preferred}} - \Delta_{\text{less-preferred}}$ becoming larger, which improves the soft-margin optimization in the loss function $L(\theta)$ that we have shown in Proof 1.

We further elaborate on why Equation 13 is true. In the context of mean squared error (MSE) minimization, the optimal predictor of $\boldsymbol{\epsilon}^l$ given some information is the conditional expectation:

- When conditioned on $(\mathbf{x}_t^l, t, c)$:

$$\boldsymbol{\epsilon}_\theta^*(\mathbf{x}_t^l, t, c) = \mathbb{E}\left[\boldsymbol{\epsilon}^l \mid \mathbf{x}_t^l, t, c\right]$$

- When conditioned on $(\mathbf{x}_t^l, t, z^l)$:

$$\boldsymbol{\epsilon}_\theta^*(\mathbf{x}_t^l, t, z^l) = \mathbb{E}\left[\boldsymbol{\epsilon}^l \mid \mathbf{x}_t^l, t, z^l\right]$$

The total variance of $\boldsymbol{\epsilon}^l$ can be decomposed as by the Law of Total Variance (conditional variance formula) (Ross, 2014):

$$\mathrm{Var}\left(\boldsymbol{\epsilon}^l\right) = \mathbb{E}\left[\mathrm{Var}\left(\boldsymbol{\epsilon}^l \mid \mathbf{x}_t^l, t, c\right)\right] + \mathrm{Var}\left(\mathbb{E}\left[\boldsymbol{\epsilon}^l \mid \mathbf{x}_t^l, t, c\right]\right)$$

Similarly, when conditioning on z^l:

$$\mathrm{Var}\left(\boldsymbol{\epsilon}^l\right) = \mathbb{E}\left[\mathrm{Var}\left(\boldsymbol{\epsilon}^l \mid \mathbf{x}_t^l, t, z^l\right)\right] + \mathrm{Var}\left(\mathbb{E}\left[\boldsymbol{\epsilon}^l \mid \mathbf{x}_t^l, t, z^l\right]\right)$$

Since $c \subset z^l$, the information provided by z^l is richer than that of c. In probability theory, conditioning on more information does not increase the conditional variance:

$$\mathrm{Var}\left(\boldsymbol{\epsilon}^l \mid \mathbf{x}_t^l, t, z^l\right) \leq \mathrm{Var}\left(\boldsymbol{\epsilon}^l \mid \mathbf{x}_t^l, t, c\right) \tag{14}$$

This inequality holds because conditioning on additional information (z^l) can only reduce or leave unchanged the uncertainty (variance) about $\boldsymbol{\epsilon}^l$.

The expected squared error when using the optimal predictor is equal to the conditional variance:

$$\mathbb{E}\left[\left\|\boldsymbol{\epsilon}^l - \boldsymbol{\epsilon}_\theta^*(\mathbf{x}_t^l, t, c)\right\|_2^2\right] = \mathbb{E}\left[\mathrm{Var}\left(\boldsymbol{\epsilon}^l \mid \mathbf{x}_t^l, t, c\right)\right]$$

Similarly,

$$\mathbb{E}\left[\left\|\boldsymbol{\epsilon}^l - \boldsymbol{\epsilon}_\theta^*(\mathbf{x}_t^l, t, z^l)\right\|_2^2\right] = \mathbb{E}\left[\mathrm{Var}\left(\boldsymbol{\epsilon}^l \mid \mathbf{x}_t^l, t, z^l\right)\right]$$

From 14, we have:

$$\mathrm{Var}\left(\boldsymbol{\epsilon}^l \mid \mathbf{x}_t^l, t, z^l\right) \leq \mathrm{Var}\left(\boldsymbol{\epsilon}^l \mid \mathbf{x}_t^l, t, c\right)$$

Taking expectations on both sides:

$$\mathbb{E}\left[\mathrm{Var}\left(\boldsymbol{\epsilon}^l \mid \mathbf{x}_t^l, t, z^l\right)\right] \leq \mathbb{E}\left[\mathrm{Var}\left(\boldsymbol{\epsilon}^l \mid \mathbf{x}_t^l, t, c\right)\right]$$

Therefore,

$$\mathbb{E}\left[\left\|\boldsymbol{\epsilon}^l - \boldsymbol{\epsilon}_\theta^*(\mathbf{x}_t^l, t, z^l)\right\|_2^2\right] \leq \mathbb{E}\left[\left\|\boldsymbol{\epsilon}^l - \boldsymbol{\epsilon}_\theta^*(\mathbf{x}_t^l, t, c)\right\|_2^2\right]$$

Assuming that the neural network $\boldsymbol{\epsilon}_\theta$ is capable of approximating the optimal predictor $\boldsymbol{\epsilon}_\theta^*$, especially as training progresses and the model capacity is sufficient, we can write:

$$\left\|\boldsymbol{\epsilon}^l - \boldsymbol{\epsilon}_\theta(\mathbf{x}_t^l, t, z^l)\right\|_2^2 \approx \left\|\boldsymbol{\epsilon}^l - \boldsymbol{\epsilon}_\theta^*(\mathbf{x}_t^l, t, z^l)\right\|_2^2$$

Similarly for c

$$\left\|\boldsymbol{\epsilon}^l - \boldsymbol{\epsilon}_\theta(\mathbf{x}_t^l, t, c)\right\|_2^2 \approx \left\|\boldsymbol{\epsilon}^l - \boldsymbol{\epsilon}_\theta^*(\mathbf{x}_t^l, t, c)\right\|_2^2.$$

Therefore, the expected squared error satisfies:

$$\mathbb{E}\left[\left\|\boldsymbol{\epsilon}^l - \boldsymbol{\epsilon}_\theta(\mathbf{x}_t^l, t, z^l)\right\|_2^2\right] \leq \mathbb{E}\left[\left\|\boldsymbol{\epsilon}^l - \boldsymbol{\epsilon}_\theta(\mathbf{x}_t^l, t, c)\right\|_2^2\right]$$

Since the term of $\Delta_{\text{less-preferred}}$ in the loss function involves the difference of squared errors, using z^l instead of c for the less preferred sample results in a lower error term:

$$\Delta_{\text{less-preferred}}^{(z^l)} = \left\|\boldsymbol{\epsilon}^l - \boldsymbol{\epsilon}_\theta(\mathbf{x}_t^l, t, z^l)\right\|_2^2 - \left\|\boldsymbol{\epsilon}^l - \boldsymbol{\epsilon}_{\text{ref}}(\mathbf{x}_t^l, t, z^l)\right\|_2^2$$

Comparing with the original:

$$\Delta^{(c)}_{\text{less-preferred}} = \left\|\boldsymbol{\epsilon}^l - \boldsymbol{\epsilon}_\theta(\mathbf{x}^l_t, t, c)\right\|_2^2 - \left\|\boldsymbol{\epsilon}^l - \boldsymbol{\epsilon}_{\text{ref}}(\mathbf{x}^l_t, t, c)\right\|_2^2$$

Assuming the reference model $\boldsymbol{\epsilon}_{\text{ref}}$ remains the same or also benefits similarly from the additional information in z^l, the net effect is that the first term decreases more than the second term, leading to a reduced $\Delta_{\text{less-preferred}}$.

Proof 3 *Replacing caption c with the specifically generated caption z^w for the preferred image $\mathbf{x}^w_0$ increases $\Delta_{preferred}$.*

To prove that replacing $\mathbf{c}$ with $\mathbf{z}^w \sim Q(z^w|x^w, c)$, where $\mathbf{c} \subset \mathbf{z}^w$, for $\mathbf{x}^w_0$ also contributes to a better optimized loss $L(\theta)$, we examine how this particular substitution affects the loss function.
We let

$$R_\theta(\mathbf{c}) = \|\boldsymbol{\epsilon}^w - \boldsymbol{\epsilon}_\theta(\mathbf{x}^w_t, t, \mathbf{c})\|_2^2,$$
$$R_{\text{ref}}(\mathbf{c}) = \|\boldsymbol{\epsilon}^w - \boldsymbol{\epsilon}_{\text{ref}}(\mathbf{x}^w_t, t, \mathbf{c})\|_2^2.$$

The rate of decrease in R_θ due to $\mathbf{z}^w$ is proportional to the model's ability to exploit the additional conditioning. Since $\boldsymbol{\epsilon}_\theta$ is learnable, it can more effectively leverage $\mathbf{z}^w$ than $\boldsymbol{\epsilon}_{\text{ref}}$, yielding:

$$\Delta R_\theta = R_\theta(\mathbf{c}) - R_\theta(\mathbf{z}^w) \gg \Delta R_{\text{ref}} = R_{\text{ref}}(\mathbf{c}) - R_{\text{ref}}(\mathbf{z}^w).$$

We further elaborate on why the learnable model's noise prediction residual (R_θ) decreases faster than the reference model's residual (R_{ref}) when $\mathbf{c}$ is replaced by $\mathbf{z}^w$. The residuals for the learnable and reference models are defined as:

$$R_\theta(\mathbf{c}) = \|\boldsymbol{\epsilon}^w - \boldsymbol{\epsilon}_\theta(\mathbf{x}^w_t, t, \mathbf{c})\|_2^2,$$
$$R_{\text{ref}}(\mathbf{c}) = \|\boldsymbol{\epsilon}^w - \boldsymbol{\epsilon}_{\text{ref}}(\mathbf{x}^w_t, t, \mathbf{c})\|_2^2.$$

When $\mathbf{c}$ is replaced with $\mathbf{z}^w$ (where $\mathbf{c} \subset \mathbf{z}^w$), the residuals become:

$$R_\theta(\mathbf{z}^w) = \|\boldsymbol{\epsilon}^w - \boldsymbol{\epsilon}_\theta(\mathbf{x}^w_t, t, \mathbf{z}^w)\|_2^2,$$
$$R_{\text{ref}}(\mathbf{z}^w) = \|\boldsymbol{\epsilon}^w - \boldsymbol{\epsilon}_{\text{ref}}(\mathbf{x}^w_t, t, \mathbf{z}^w)\|_2^2.$$

The rate of decrease for each residual is defined as:

$$\Delta R_\theta = R_\theta(\mathbf{c}) - R_\theta(\mathbf{z}^w),$$

$$\Delta R_{\text{ref}} = R_{\text{ref}}(\mathbf{c}) - R_{\text{ref}}(\mathbf{z}^w).$$

The quality of conditioning, $Q(\mathbf{c})$, represents how well the conditioning $\mathbf{c}$ aligns with the true noise $\boldsymbol{\epsilon}^w$. We assume that

$$Q(\mathbf{z}^w) > Q(\mathbf{c}),$$

where the improvement in conditioning quality ΔQ is defined as

$$\Delta Q = Q(\mathbf{z}^w) - Q(\mathbf{c}).$$

The residual for R_θ is proportional to the misalignment between $Q(\mathbf{c})$ and $\boldsymbol{\epsilon}^w$:

$$R_\theta(\mathbf{c}) \propto \frac{1}{Q(\mathbf{c})}.$$

Replacing $\mathbf{c}$ with $\mathbf{z}^w$ (higher Q) results in a larger proportional reduction:

$$R_\theta(\mathbf{z}^w) \propto \frac{1}{Q(\mathbf{z}^w)} \quad \text{with} \quad \Delta R_\theta \propto \Delta Q.$$

The reference model's residual R_{ref} depends weakly on $Q(\mathbf{c})$, as it is fixed or less adaptable:

$$R_{\text{ref}}(\mathbf{c}) \propto \frac{1}{Q_{\text{ref}}(\mathbf{c})},$$

where $Q_{\text{ref}}(\mathbf{c})$ is less sensitive to changes in $\mathbf{c}$.
Thus, the proportional improvement in R_θ due to ΔQ is significantly larger than for R_{ref}.
The preferred difference term is:

$$\Delta_{\text{preferred}} = R_\theta - R_{\text{ref}}.$$

As R_θ decreases significantly more than R_{ref}, the gap $R_\theta - R_{\text{ref}}$ becomes larger, increasing $\Delta_{\text{preferred}}$:

$$\Delta R_\theta \gg \Delta R_{\text{ref}} \implies \Delta_{\text{preferred}} \text{ increases.}$$

The learnable model $\boldsymbol{\epsilon}_\theta$ benefits more from the improved conditioning $\mathbf{z}^w$ because of its adaptability and training dynamics. This results in a larger reduction in R_θ compared to R_{ref}. Mathematically, the relative rate of decrease:

$$\text{Relative Rate} = \frac{\Delta R_\theta}{\Delta R_{\text{ref}}} \gg 1,$$

which ensures that $\Delta_{\text{preferred}}$ also increases, hence improving the optimization process in $L(\theta)$ and helping the model distinguish predictions on preferred and less preferred image-captions more effectively.

C Additional Experiments and Analyses on DCPO

A preference alignment dataset, such as Pick-a-Pic (Kirstain et al., 2023), is defined as $D = \{c, x^w, x^l\}$, where x^w and x^l represent the preferred and less preferred images for the prompt c. Diffusion-KTO (Li et al., 2024) hypothesizes the optimization of a diffusion model using only a single preference label based on whether an image x is suitable or not for a given prompt c. Diffusion-KTO uses a differently formatted input dataset $D = \{c, x\}$, where x is a generated image corresponding to the prompt c.

Diffusion-KTO's hypothesis is fundamentally different from our DCPO's. While Diffusion-KTO focuses on binary preferences (like/dislike) for individual image-prompt pairs, our approach involves paired preferences. We observe that using the same prompt c for both preferred and less preferred images may not be ideal. To address this, we propose optimizing a diffusion model using a dataset in terms of $D = \{z^w, z^l, x^w, x^l\}$, where z^w and z^l are the captions generated by a static captioning model Q_ϕ for the preferred and less preferred images, respectively, referring to the original prompt.

Method	Pair Caption	Perturbed Level	Pickscore (↑)	HPSv2.1 (↑)	ImageReward (↑)	CLIPscore (↑)	GenEval (↑)
DCPO-p	(c, c_p)	weak	20.28	25.42	54.20	26.98	0.4906
DCPO-h	(z^w, z_p^w)	weak	20.55	25.61	57.70	27.07	**0.5070**
DCPO-h	(z^w, z_p^l)	weak	**20.58**	**25.70**	**58.10**	**27.15**	0.5060
DCPO-p	(c, c_p)	medium	20.21	25.34	53.10	26.87	0.4852
DCPO-h	(z^w, z_p^w)	medium	**20.59**	**25.73**	**58.47**	27.12	0.5008
DCPO-h	(z^w, z_p^l)	medium	20.57	25.62	58.20	**27.13**	**0.5100**
DCPO-p	(c, c_p)	strong	20.31	25.06	54.60	27.03	0.4868
DCPO-h	(z^w, z_p^w)	strong	20.57	25.27	57.43	27.18	**0.5110**
DCPO-h	(z^w, z_p^l)	strong	**20.58**	**25.43**	**57.90**	**27.21**	0.4993

Table 3: Performance comparison of DCPO-h and DCPO-p across different perturbation levels. The perturbation method has a strong impact on captions that are more closely correlated with images.

Method	Input Prompt	Token Length (Avg)	Pickscore (↑)	HPSv2.1 (↑)	ImageReward (↑)	CLIPscore (↑)	GenEval (↑)
Diffusion-DPO	prompt c	15.95	20.36	25.10	56.4	26.98	0.4857
Diffusion-DPO	caption z^w (LLaVA)	32.32	20.40	25.19	56.6	27.10	0.4958
Diffusion-DPO	caption z^w (Emu2)	7.75	20.36	25.08	56.3	26.98	0.4960
DCPO-h (LLaVA)	Pair (z^w,z_p^l)	(32.32, 31.17)	**20.57**	**25.62**	**58.2**	27.13	0.5100
DCPO-h (LLaVA)	Pair (z^w,z_p^w)	(32.32, 27.01)	**20.57**	25.27	57.4	**27.18**	**0.5110**

Table 4: Performance comparison of DCPO and Diffusion-DPO fine-tuned on the *Pick-Double Caption* dataset. While larger captions improve the performance of Diffusion-DPO, DCPO-h still significantly outperforms Diffusion-DPO.

Method	GenEval (↑)	Pickscore (↑)	HPSv2.1 (↑)	ImageReward (↑)	CLIPscore (↑)
Diffusion-KTO	0.5008	20.41	24.80	55.5	26.95
DCPO-h	**0.5100**	**20.57**	**25.62**	**58.2**	**27.13**

Table 5: Comparison of DCPO-h and Diffusion-KTO across various benchmarks.

We nonetheless conduct comparisons between Diffusion-KTO and DCPO on various preference alignment benchmarks. The results in Table 5 show that our DCPO-h consistently outperforms Diffusion-KTO on all benchmarks, demonstrating the effectiveness of our DCPO method.

To further demonstrate DCPO's versatility, we fine-tune Stable Diffusion 2.1 using Diffusion-DPO and DCPO on another high-quality preference dataset Rapidata (Christodoulou and Kuhlmann-Jørgensen, 2024). Table 6 shows that our DCPO variants consistently outperform the Diffusion-DPO baseline on multiple benchmarking metrics, including GenEval, Pickscore, HPSv2.1, ImageReward, and CLIPscore.

Method (SD2.1)	Geneval	Pickscore	HPSv2.1	ImageReward	CLIPscore
Diffusion-DPO	0.4813	20.34	25.10	55.4	26.84
DCPO-c	0.4867	**20.44**	**25.43**	**55.7**	26.86
DCPO-h	**0.4978**	20.42	25.10	55.6	**26.91**

Table 6: DCPO performances using SD2.1 on Rapidata (Christodoulou and Kuhlmann-Jørgensen, 2024).

We also perform additional experiments to evaluate the performance of DCPO using Stable Diffusion XL (SDXL) (Podell et al., 2023), a different backbone model for T2I. Due to the larger parameter size of SDXL, we conduct LoRA fine-tuning with minimal hyperparameter search. The results in Table 7 show that DCPO outperforms Diffusion-DPO on key metrics such as Pickscore, Geneval, HPSv2, and CLIPscore, while achieving comparable performance on ImageReward. We hope that our results would encourage other researchers to further explore DCPO's effectiveness on different datasets in future, gaining more valuable insights into its broader applicability and robustness.

D Pick-Double Caption Dataset

In this section, we provide details about the *Pick-Double Caption* dataset. As discussed in Section 4.1, we sampled 20,000 instances from the Pick-a-Pic v2 dataset and excluded those with equal preference scores. We plot the distribution of the original prompts, as shown in Figure 8.

We observed that some prompts contained only one or two words, while others were excessively long. To ensure a fair comparison, we removed prompts that were too short or too long, leaving us with approximately 17,000 instances. We then generated captions using two state-of-the-art models, LLaVA-1.6-34B, and Emu2-32B. The construction of the *Pick-Double Caption* dataset is illustrated in Figure 9, which provides several examples.

We acknowledge that while captioning and perturbation introduce additional computational costs, these are one-time expenses incurred only during pre-processing and do not affect training or evaluation time. We introduce three variants of DCPO—c, p, and h—each with different processing requirements. For instance, DCPO-c and DCPO-h involve captioning, whereas DCPO-p is more computationally efficient as it only perturbs a less preferred caption. Furthermore, captioning 20,000 images using LLaVA

Method (SDXL)	Geneval (Overall)	Pickscore	HPSv2.1	ImageReward	CLIPscore
Diffusion-DPO	0.5645	21.77	28.64	71.2	28.61
DCPO-c	**0.5758**	**21.87**	**28.65**	71.2	**28.63**
DCPO-h-weak	0.5704	**21.87**	28.64	71.2	28.62
DCPO-h-medium	0.5700	21.86	28.64	71.2	**28.63**
DCPO-h-strong	0.5696	21.86	28.64	71.2	28.62

Table 7: DCPO performances of using Stable Diffusion XL (SDXL) (Podell et al., 2023) as the backbone model.

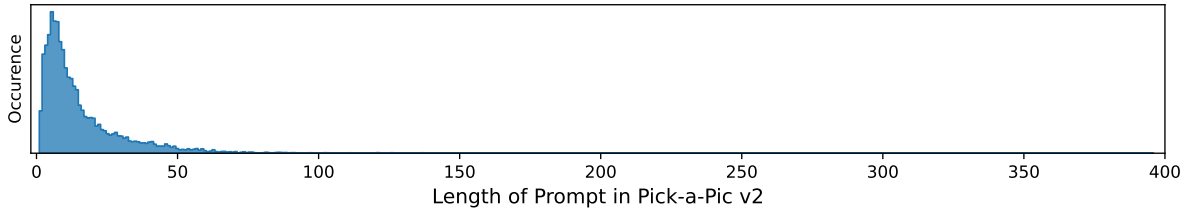

Figure 8: The distribution of token lengths in the original prompts.

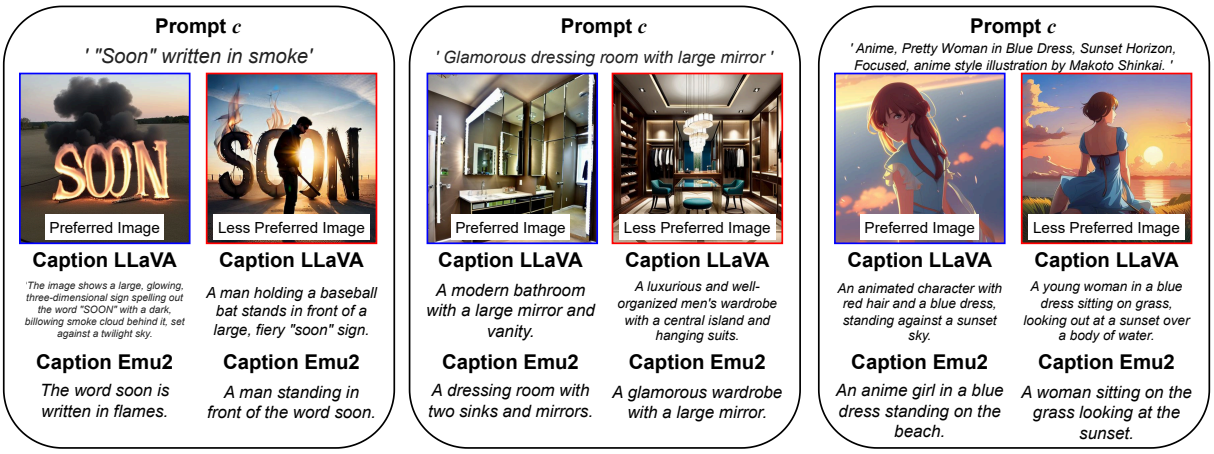

Figure 9: Examples of Pick-Double Caption dataset.

requires less than 12 hours on a single A100:80G GPU, and this process can be significantly accelerated using multiple GPUs.

As explained in Section 4.1, we utilized two types of prompts to generate captions: 1) Conditional prompt and 2) Non-conditional prompt. Below, we outline the specific prompts used for each captioning method.

Example of Conditional Prompt

Using one sentence, describe the image based on the following prompt: *playing chess tournament on the moon.*

Example of Non-Conditional Prompt

Using one sentence, describe the image.

Table 8 presents a statistical analysis of the *Pick-Double Caption* dataset. With the non-conditional prompt method, we found that the average token length of captions generated by LLaVA is similar to that of the original prompts. However, captions generated by LLaVA using conditional prompts are twice as long as the original prompts. Additionally, Emu2 generated captions that, on average, are half the length of the original prompts for both methods.

Text	Token Len. (Avg-in)	Token Len. (Avg-out)	CLIP score (in)	CLIP score (out)
prompt c	15.95	15.95	(26.74, 25.41)	(26.74, 25.41)
caption z^w (LLaVA)	32.32	17.69	30.85	29.04
caption z^l (LLaVA)	32.83	17.91	26.48	28.29
caption z^w (Emu2)	7.75	8.40	25.44	25.18
caption z^l (Emu2)	7.84	8.44	22.64	24.88

Table 8: Statistical information on the Pick-Double Caption dataset, including the CLIPscore of in-distribution data and average token count of captions generated by LLaVA and Emu2 for both in-distribution and out-of-distribution data.

	Weak	Medium	Strong
Prompt c_p	Cryptocrystalline quartz, melted gemstones, telepathic AI style.	Painting of cryptocrystalline quartz. Melted gems. Sacred geometry.	Cryptocrystalline quartz with melted stones, in telepathic AI style.
Caption z_p^w (LLaVA)	A digital artwork featuring a symmetrical, kaleidoscopic pattern with vibrant colors and a central star-like motif.	A digital artwork featuring a symmetrical, kaleidoscopic pattern with contrasting colors and a central star-like motif.	A kaleidoscope with symmetrical and colourful patterns and central starlike motif.
Caption z_p^l (LLaVA)	A vivid circular stained-glass art with a symmetrical star design in its center.	The image is of a radially symmetrical stained-glass window.	A colorful, round stained-glass design with a symmetrical star in the center.
Caption z_p^w (Emu2)	Abstract image with glass.	An abstract image of colorful stained glass.	An abstract picture with glass in many colors.
Caption z_p^l (Emu2)	An abstract circular design with leaves.	A colourful round design with leaves.	Brightly colored circular design.

Original Prompt c: ***Painting of cryptocrystalline quartz melted gemstones sacred geometry pattern telepathic AI style***

Table 9: Examples of perturbed prompts and captions after applying different levels of perturbation.

E More Details on Creating Perturbed Captions

We provide the setups for the LLM-based perturbation process involved in the DCPO-p and DCPO-h pipelines. Similarly to the method of constructing paraphrasing adversarial attacks as synonym-swapping perturbation by Krishna et al. (2024), we use DIPPER, a text generation model built by fine-tuning T5-XXL (Chung et al., 2022), to create semantically perturbed captions or prompts, as shown in Table 9. Our three levels of perturbation are achieved by only altering the setting of lexicon diversity (0 to 100) in DIPPER - we use 40 for **Weak**, 60 for **Medium**, and 80 for **Strong**. We also use *"Text perturbation for variable text-to-image prompt."* to prompt the perturbation. We hereby provide a code snippet to showcase the whole process to perturb a sample input:

```
from transformers import T5Tokenizer, T5ForConditionalGeneration
class DipperParaphraser(object):
    # As defined in https://huggingface.co/kalpeshk2011/dipper-paraphraser-xxl

prompt = "Text perturbation for variable text-to-image prompt."
input_text = "playing chess tournament on the moon."

dp = DipperParaphraser()

cap_weak = dp.paraphrase(input_text, lex_diversity=40, prefix=prompt, do_sample=True
    , top_p=0.75, top_k=None, max_length=256)
cap_medium = dp.paraphrase(input_text, lex_diversity=60, prefix=prompt, do_sample=
    True, top_p=0.75, top_k=None, max_length=256)
cap_strong = dp.paraphrase(input_text, lex_diversity=80, prefix=prompt, do_sample=
    True, top_p=0.75, top_k=None, max_length=256)
```

F More Details about Training of Diffusion Models

In this section, we provide a detailed explanation of the fine-tuning methods used. We fine-tuned SD 2.1 with the best hyperparameters reported in the original papers for $\text{SFT}_{\text{Chosen}}$, Diffusion-DPO, and MaPO,

Method	Pair Caption	Perturbed Level	Pickscore (↑)	HPSv2.1 (↑)	ImageReward (↑)	CLIPscore (↑)	GenEval (↑)
DCPO-h	(z^w, z_p^w)	weak	20.10	21.23	49.7	26.87	0.5003
DCPO-h	(z^w, z_p^l)	weak	20.32	23.4	53.8	27.06	0.5070
DCPO-h	(z^w, z_p^w)	medium	20.31	23.08	53.2	27.01	0.4895
DCPO-h	(z^w, z_p^l)	medium	20.33	23.22	53.8	27.09	0.5009
DCPO-h	(z^w, z_p^w)	strong	20.31	22.95	53.1	27.11	0.4878
DCPO-h	(z^w, z_p^l)	strong	20.35	23.24	53.63	27.08	0.5050

Table 10: Results of the perturbation method applied to Emu2 captions across different levels.

Method	β	Pickscore (↑)	HPSv2.1 (↑)	ImageReward (↑)	CLIPscore (↑)	GenEval (↑)
DCPO-h	500	20.43	**26.42**	58.1	27.02	**0.5208**
DCPO-h	1000	20.51	26.12	**58.2**	27.10	0.4900
DCPO-h	2500	20.53	25.81	58.0	27.02	0.5036
DCPO-h	5000	**20.57**	25.62	**58.2**	**27.13**	0.5100

Table 11: Results of DCPO-h across different β.

using 8 A100 80 GB GPUs for all models. To fine-tune SD 2.1 with Diffusion and MaPO methods, we used a dataset $D = \{c, x^w, x^l\}$ where c, x^w, x^l represent the prompt, preferred image, and less preferred image. To optimize a SD2.1 with $\text{SFT}_{\text{Chosen}}$ we utilized a dataset $D = \{c, x^w\}$ where c, x^w represent the prompt, preferred image and image. In this paper, dataset D represents the sampled and cleaned version of the Pick-a-Pic v2 dataset. Additionally, we clarify the DCPO models DCPO-c, DCPO-p, and DCPO-h. In this paper, DCPO-c and DCPO-p refer to SD 2.1 models fine-tuned with the DCPO method, using LLaVA and Emu2 for captioning and perturbation methods at three distinct levels, respectively. The main results for DCPO-p in the text are based on weak perturbation applied to the original prompt. In Table 3, we also report DCPO-p's performance across other perturbation levels.

For DCPO-h, we applied perturbations to both the preferred and less preferred captions generated by LLaVA. The reported results for DCPO-h reflect a medium level of perturbation applied to the less preferred caption. In Table 3, we present the performance of DCPO-h across various perturbation levels, including perturbations to the preferred captions. Additionally, in Table 10, we show the results for DCPO-h using captions generated by Emu2.

The key findings indicate that perturbation on short captions not only fails to improve performance but also produces worse outcomes compared to DCPO-c (Emu2).

Additionally, we conducted more experiments on in-distribution and out-of-distribution data. For this, we generated out-of-distribution data using LLaVA and Emu2 in the captioning setup. As shown in Figure 10, in-distribution data generally outperformed out-of-distribution data. However, the most significant improvement was observed with the hybrid method, as reported in Figure 6.

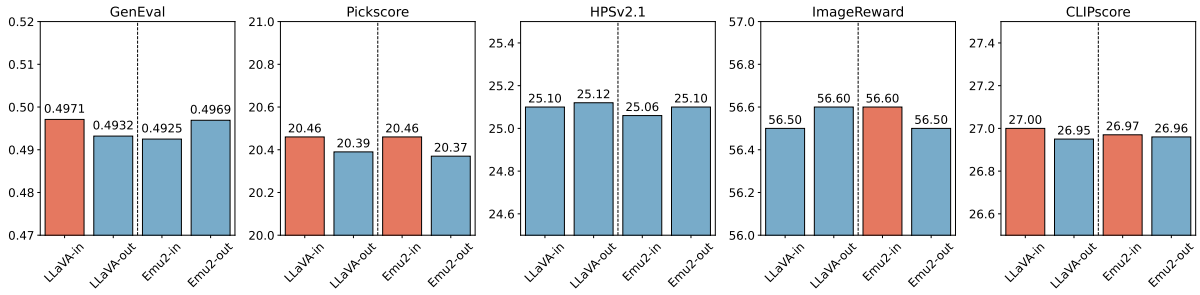

Figure 10: Comparison of DCPO-c performance on in-distribution and out-of-distribution data.

Table 11 presents the performance details for different values of β, conducted using the medium level of DCPO-h. The results indicate that while lower values of β significantly improve GenEval and HPSv2.1 on average, the optimal value for β is 5000. We suggest that this hyperparameter may vary based on the dataset and task.

Method	General Preference	Visual Appeal	Prompt Alignment
DCPO-h	**58%**	**64.5%**	**56.5%**
Diffusion-DPO	42%	35.5%	43.5%

Table 12: Comparison of DCPO and Diffusion-DPO across different positions based on various criteria.

G GPT-4o as Evaluator

To obtain binary preferences from the API evaluator, we follow the approach outlined in the MaPO paper (Hong et al., 2024). To address positional bias in GPT-4o's evaluations, we alternate the positions of the images across different criteria on 100 samples (explained in Section 4). The results in Table 12 show that DCPO consistently achieves better performance than Diffusion-DPO, even when positional bias is accounted for.

Similarly to Diffusion-DPO, we use three distinct questions to evaluate the images generated by DCPO-h and other baseline models, all utilizing SD 2.1 as the backbone. These questions are presented to GPT-4o to identify the preferred image. In the following, we provide details of the prompts used.

GPT-4o Evaluation Prompt for Q1: General Preference

Select the output (a) or (b) that best matches the given prompt. Choose your preferred output, which can be subjective. Your answer should ONLY contain: Output (a) or Output (b).

Prompt:
`{prompt}`

Output (a):
The first image attached.

Output (b):
The second image attached.

Which image do you prefer given the prompt?

GPT-4o Evaluation Prompt for Q2: Visual Appeal

Select the output (a) or (b) that best matches the given prompt. Choose your preferred output, which can be subjective. Your answer should ONLY contain: Output (a) or Output (b).

Prompt:
`{prompt}`

Output (a):
The first image attached.

Output (b):
The second image attached.

Which image is more visually appealing?

GPT-4o Evaluation Prompt for Q3: Prompt Alignment

Select the output (a) or (b) that best matches the given prompt. Choose your preferred output, which can be subjective. Your answer should ONLY contain: Output (a) or Output (b).

Prompt:
`{prompt}`

Output (a):
The first image attached.

Output (b):
The second image attached.

Which image better fits the text description?

H Additional Generation Samples

We also present additional samples for qualitative comparison generated by SD 2.1, $\text{SFT}_{\text{Chosen}}$, Diffusion-DPO, MaPO, and DCPO-h from prompts on Pickscore, HPSv2, and GenEval benchmarks.

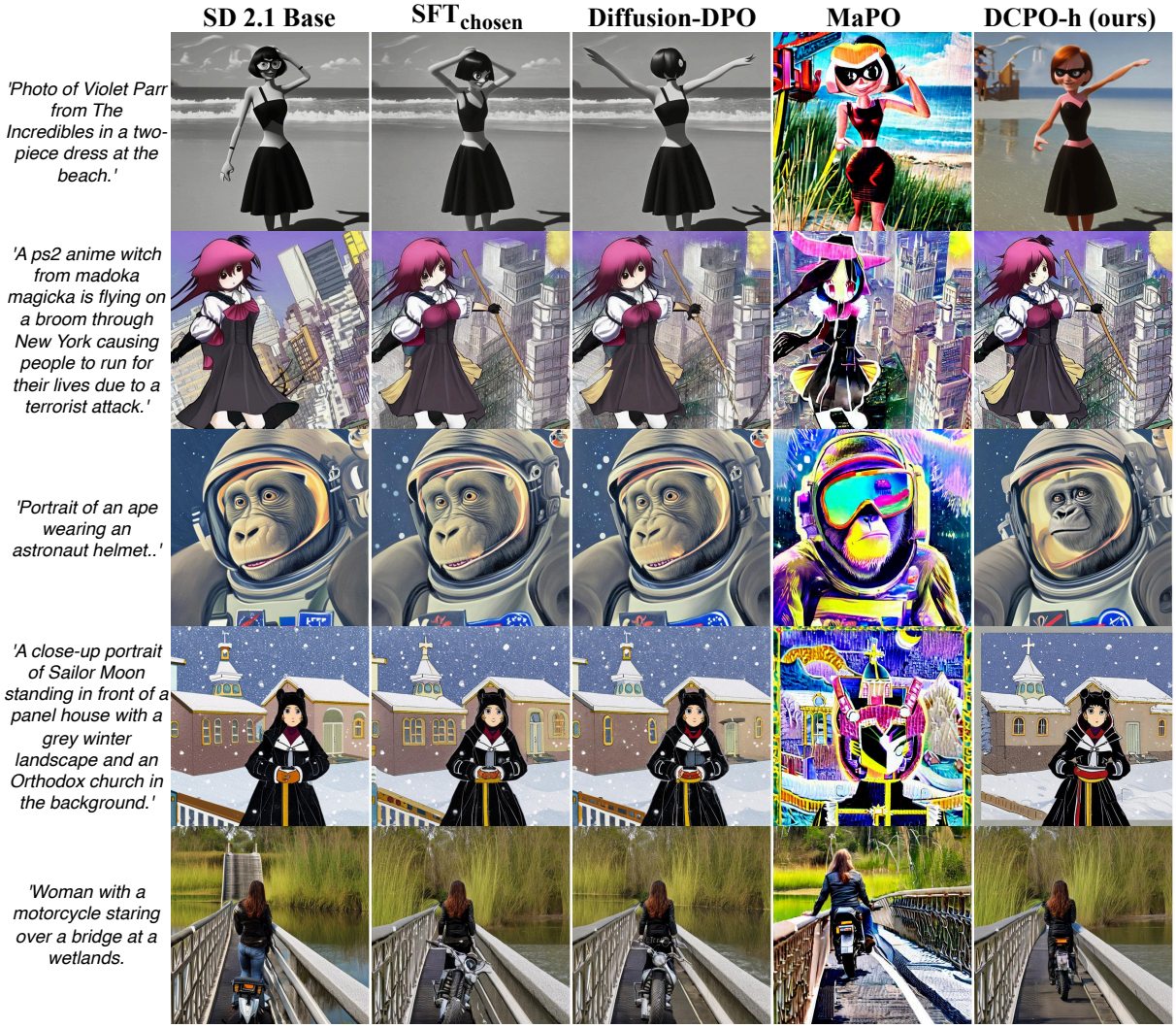

Figure 11: Additional generated outcomes using prompts from HPSv2 benchmark.

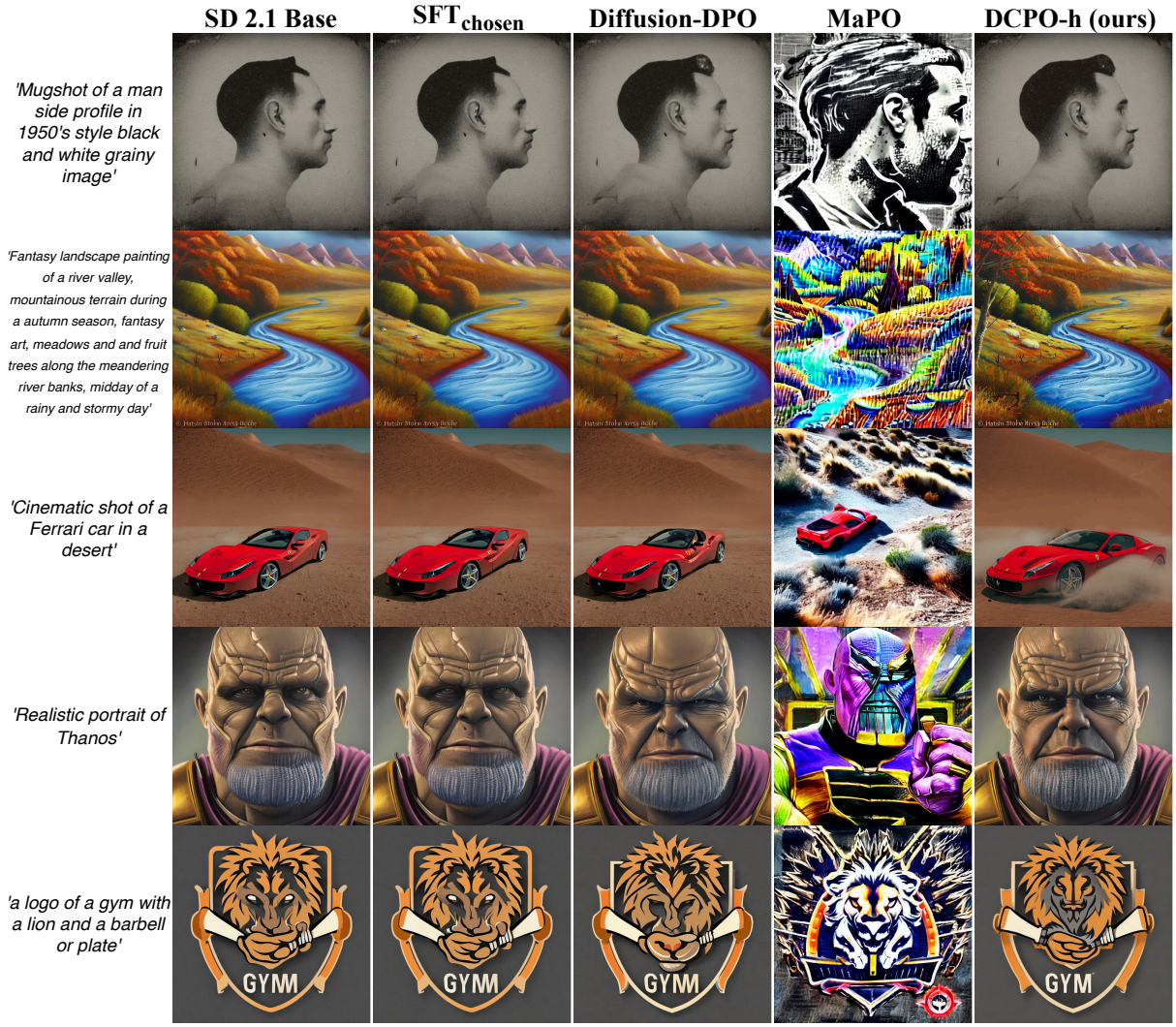

Figure 12: Additional generated outcomes using prompts from Pickscore benchmark.

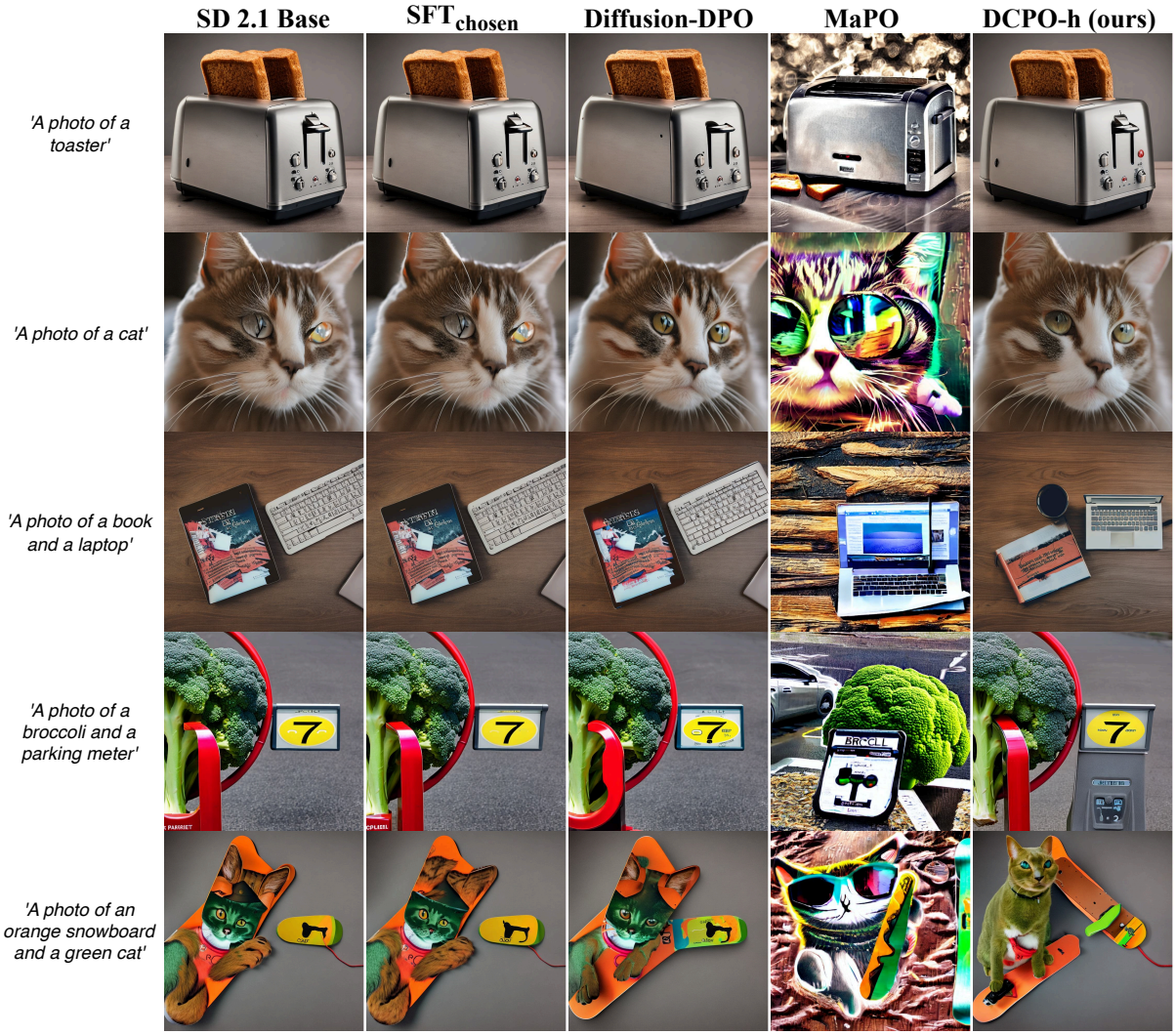

Figure 13: Additional generated outcomes using prompts from GenEval benchmark.